universität wien

MASTERARBEIT / MASTER'S THESIS

Titel der Masterarbeit /Title of the Master's Thesis

Induction heating of exoplanets on eccentric orbits around M dwarfs

verfasst von / submitted by

Daniela Maria Dittrich Bakk. rer. nat.

angestrebter akademischer Grad / in partial fulfilment of the requirements for the degree of

Master of Science (MSc)

Wien, 2018 / Vienna, 2018

Studienkennzahl lt. Studienblatt / degree programme code as it appears on the student record sheet:	A 066861
Studienrichtung lt. Studienblatt / degree programme as it appears on the student record sheet:	Astronomie
Betreuerin / Supervisor:	Dr. Kristina G. Kislyakova

‚In the vastness of space

and

the immensity of time,

it is my joy

to share planet and an epoch with Anni'

(Carl Sagan)

Introduction

The stellar magnetic field influences the planet in many way, for example, more active stars with stronger fields usually have higher XUV radiation levels, which influence the atmospheres (Zahnle and Walker 1982, Lammer et al. 2008 & 2009). The strength of the stellar magnetic field is determined by the stellar formation process. The onset of star formation is a rotating interstellar gas cloud formed by contraction and acting centrifugal forces into a highly flattened structure. In this protoplanetary disk the star is formed in the center. Energetic radiation of the forming host star ionizes disk matter, while magnetic fields transmit the original angular momentum of the star to the plasma in the disk. As a result, the disk is accelerated, flattened and spread apart, whereby the stellar rotation decelerates. If the relative velocity of roughly equal mass particles in the disk is small enough, they can adhere to one another without evaporation due to the impact energy. Through this so-called coagulation numerous bodies with a size of 1 to 10 km arise, which are referred to as planetesimals. Under the influence of gravitational interactions, a protoplanet is formed. Finally, the formation of the planet and possible moons occurs (Weigert et al. 2006, p. 101-102).

With the increasing sensitivity of observational instruments, ever since the first discovery of an exoplanet at the beginning of the 1990s (Wolszczan and Frail 1992, Mayor and Queloz 1995), more and more small, potentially Earth-like, rocky planets have been detected (Charbonneau et al. 2009, Borucki et al. 2011). Some planets, such as Kepler-10b and CoRoT-7b, have high average densities indicative of the presence of a large iron core in the interior (Wagner et al. 2012).

Many conditions have to be fulfilled in order to enable the emergence of life on a planet and subsequent millions of years of habitability. The appropriate distance from the central star is important for the planet to receive the right amount of the stellar energy to provide a temperate surface temperature and allow the water to be in its liquid form (Seager 2013, Guedel et al. 2014). The need for the presence of water in liquid form refers to the fact that the emergence or survival of life as we know it is dependent on liquid water. Due to the limited ability to obtain accurate information about the subsurface conditions, the concept of habitability is generally defined by the presence of liquid water on the planet's rocky surface (Hart 1979, Kasting et al. 1993, Kopparapu et al. 2013, Rogers 2015). Several potential factors for habitat depend on the creation and maintenance of a planetary atmosphere. The atmospheric pressure affects the phase transition of water and is able to protect the surface from micrometeorite impacts. About 90% of the extraterrestrial material, which penetrates into the exosphere of our planet in the form of micrometeorites, evaporates before it reaches the ground (Peucker−Ehrenbrink & Ravizza 2000, Grenfell et al. 2010). Depending on the thickness, the atmosphere is able to protect the surface from particles and radiation from the outside (Dartnell 2011). UV radiation can be very destructive. Different cell components and DNA are attacked and harmed by UV photons (Bonura & Smith 1975a, b).

To create a habitat in the long term, the presence of nutrients such as the elements of CHNOPS (carbon, hydrogen, nitrogen, oxygen, phosphorous and sulfur) is just as crucial as the existence of a magnetic field. The magnetosphere of a planet can preserve the surface from penetration by cosmic rays and other high energy particles (Horneck et al. 2016, Lundin et al. 2007). To determine to what extent the conditions of life on a rocky exoplanet depend on

stellar evolution, the spectrum of the star, as well as the resulting radiation flux, is one of the major goals of exoplanetary missions like PLATO 2.0 (Rauer et al. 2014). Studies of the Earth help us to understand to what extent plate tectonics is required to maintain the habitability of an extrasolar planet (Southam et al. 2015). In the solar system, of all the terrestrial planets and moons, only the Earth exhibits plate tectonics (Noack et al. 2012, Turcotte 1993). Active plate tectonics is essential in maintaining a periodic, geochemical transformation, the carbon-silicate cycle. The carbon-silicate cycle is considered to be a crucial regulator of atmospheric carbon content over long periods of time, positively affecting the stability of the climate (Walker et al. 1981, Kasting et al. 1993). The focus in exploration of exoplanets lies in the discovery of rocky planets within the habitable zone. At present, there are no methods able to determine remotely if an exoplanet has an active plate tectonics or is in the stagnant lid regime. Stagnant lid, probably the most abundant tectonic mode in terrestrial planets and moons in the solar system, is based on the strong dependence of the planet's mantle viscosity on temperature (Christensen 1984, Davaille & Jaupart 1993, Solomatov 1995, Tosi et al. 2017).

The search for new planets in the stellar habitable zones has aroused the interest of many scientists for years. A habitable zone's planet could be inhabitable because of its enhanced greenhouse effect, like Venus. On the other hand, it is also possible that a planet in this area has a high albedo, causing the planet's surface to reflect too much light and thus be too cold to host life (Grimm et al. 2018). In exploring whether a planet could be habitable, studying and describing its interior in its present-day state and its evolution in time is of crucial importance. There are different types of planets. For solid, which are also called rocky or terrestrial planets, the composition of the main building materials iron, silicate and water is assumed. Depending on the mass, the density and the initial water content, exoplanets exist in manifold variations (Valencia et al 2007, Zeng & Seager 2008). The differentiation of a rocky exoplanet describes the formation of a silicate mantle surrounding an iron core by gravitational separation and chemical affinities. Due to the higher density, iron is transported to the planet's interior. By sinking to the core, the metal can melt and release potential energy. In addition, if enough heat of the kinetic energy from the accretion phase of the planet is stored in the interior, the outer core and mantle areas may be in a viscous or liquid state (Rubie et al. 2003; Terasaki et al. 2005; Jacobsen 2005).

In addition to the major internal heating source, radiative decay, if enough heat from the kinetic energy from the accretion phase of the planet could be stored inside, the outer core and mantle areas are in a viscous or liquid state. This leads to global convection in these two layers. The solid and liquid nuclei create a dynamo that forms a magnetic field around the planet. In the case of Earth, this is called geodynamo. The planet-wide circulation in the outer silicate mantle is responsible for the conservation of plate tectonics at Earth (Shirey & Richardson 2011).

In the case of gas giants, such as Jupiter and Saturn, the magnetic field is driven by an electrically conductive metallic hydrogen layer inside the planet. A dynamo transforms the kinetic energy of charged particles into magnetic energy. Since eddy currents are generated by the movement of an electrically conductive fluid, a magnetic field is created. In addition to convection, which is a significant influence, librational, nutational and tidal interactions also affect the dynamo processes (Schubert & Soderlund 2011). Because a planet is a dynamic object, heating or cooling processes and related effects such as motions and melting and solidification of interiors lead to changes in internal properties.

The thermal energy and the heat transport of a celestial body are also determined by the sources of heat. An original heat comes from the planet's time of creation, when many planetesimals grow into a larger object through collisions, their kinetic energy is converted to heat. Another source of heat are radioactive elements. Rocky planets have a trace amounts of radioactive elements that, through decay processes, heat up the celestial body over time. The heat transport ensures the transmission and equalization of temperatures in and around a body. Conduction, radiative transfer and convection are the three ways to transport heat. For being able to make estimates for the conductivity of different planet layers, data about the rock composition are necessary. The occurrence of the most important radioactive elements known to us, such as uranium, potassium and thorium in the planet must be estimated (Hartmann 1983, p. 262-263).

Several mechanisms of internal energy production in a planet are known to date. Sources of heat generation include core and inner core formation, mantle differentiation (Rubie et al. 2003, Terasaki et al. 2005, Jacobsen 2005), radioactive decay (Hartmann 1983, p. 262-263), tidal heating (Dole 1964, Kasting et al. 1993) and induction heating (Schwartz, Sonett, Colburn and 1969). For Earth, the last two mechanisms are not important (Patiño Douce 2011). Exoplanets that orbit M dwarfs, however, may be strongly influenced by the effects of tidal and induction heating (Doyle et al. 1993, Kislyakova et al. 2017 & 2018). If a planetary body has a small orbit around a central body, tidal forces are significant. The main heat source of Juipter's nearby moon Io is tidal heating, which makes Io the most active volcanic body in the solar system (Goldreich & Lynden-Bell 1969, Colburn 1980). The amount of internal energy that can be generated by induction heating in exoplanets has so far been insufficiently researched. Based on the current investigations for the development of induction heating in planets by Kislyakova et al. 2017 & 2018, I would like to shed more light on this topic with this work.

Interest in exoplanets orbiting M dwarfs has increased significantly in recent years. M dwarfs are the largest star population in our galaxy. Their small size provides a good contrast for the detection of planets in transit searches. In addition, M stars are low-mass objects. From a terrestrial planet generated reflex motions of the star can be determined by the increasing spectroscopic sensitivity of the radial velocity searches (Kasting et al 1993, Selsis et al., 2007). Among others, three projects in the search for exoplanets orbiting M-stars: the radial velocity program using the Keck (Marcy et al., 1998) and the Hobby-Eberly telescope (Endl et al., 2003) and the astrometric program Stellar Planet Survey (STEPS) have already been able to elicit some information about M dwarf systems (Pravdo et al. 2004, 2005).

The habitable zone, the area with the potential for the emergence of life, is very close to these low-luminous stars (Kasting et al 1993, Selsis et al., 2007). If these long-lived M dwarfs host planets in their nearby habitable zone, a few additional factors may have an impact on the planet's habitats (Scalo et al., 2007, Lammer et al., 2009). Due to the small distance of the habitable zone to the M dwarf many planets in this area are tidally locked (Dole, 1964, Kasting et al., 1993). In this so-called synchronous rotation extreme temperature differences can occur on the planetary surface as only one hemisphere faces the star. Detailed climate simulations show that a tidally locked planets can still potentially be habitable. It is likely that even a moderately dense atmosphere is already able to provide efficient heat transfer to the other, the dark side of the planet (Haberle et al., 1996; Joshi et al., 1997; Joshi, 2003).

The influence of stellar ejecta and stellar radiation on potentially habitable planets in these systems have been studied thoroughly (Khodachenko et al. 2007, Lammer et al 2007, Grießmeier et al. 2005 & 2009). In particular, fast-rotating M dwarfs are likely to produce stellar winds that, when interacting with planets without a protective magnetic field, can lead to significant habitat-related impacts (Vidotto et al., 2011b). Unprotected planetary atmospheres in such systems could be fully eroded in a short time due to strong stellar winds (Zendejas et al., 2010). Some planets create their own magnetic fields. Earth-like planets are made up of a metallic core and a silicate mantle. The convection of the liquid core of these planets generates their magnetic field (Schubert & Soderlund 2011).

Already a few decades ago, the radio emissions originating from Jupiter could be attributed to an interaction with the strong magnetosphere of the gas giant (Carr & Gulkis 1969). Since then, the possibilities of observation by remote sensing and in situ measurements have improved significantly. In the solar system, besides Earth, magnetic fields of such bodies as Mercury, Ganymede, and all gas giants have been detected. In the case of the Moon and Mars, the remnant magnetization is considered to be the remnant of an active dynamo and a magnetic field in the earlier history of evolution (Stevenson 2010, Schubert & Soderlund 2011).

If a rocky planet has a strong magnetic field, this indicates the presence of a liquid core in its interior. Also the absence of a field makes it possible to make conclusions about the inner composition via near-surface magnetic observations (Hartmann 1983, p. 255). Since 1995, the Jupiter moons Io, Europe, Ganymede and Callisto have been examined more closely. Magnetometer measurements of the Galileo spacecraft showed a magnetic field generated by Ganymede (Kivelson 1996) and probably also by Io (Kivelson et al. 1996), but no significant magnetic fields of Europe and Callisto were to be measured (Kivelson et al. 1997, Khurana 1996). However, Europe and Callisto cause magnetic disturbances within the magnetosphere of Jupiter when they come too close to Io and Ganymede. It is believed that these disturbances are caused by induced magnetic fields caused by the periodic variability of the external magnetic field of Jupiter. This electromagnetic induction would require that electrically conductive layers be present below the surface of Europe and Callisto. Due to the high levels of electrical conductivity, both Jupiter moons are expected to have sub-surface water oceans that have a very high salt content (Carr et al. 1998, Pappalardo et al. 1998).

Planets close to stars seem to have an other important effect on habitability - strong, varying magnetic field can create induction heating in the planet which could cause subsurface oceans of magma (Grimm et al. 2018, Kislyakova et al. 2017 & 2018). The aim of this work is to investigate the formation of induction heating in the mantle of an Earth-like planet orbiting a magnetic active M dwarf on an eccentric orbit within the habitable zone.

In general, M dwarfs are much more active than stars that resemble the sun. It is very difficult to estimate the resulting consequences for the formation and evolution of life on a planet orbiting an M star (Gershberg et al. 1999). The outer convective zone of an M dwarf is much deeper than that of sun-like stars, creating a strong magnetic field. The associated high levels of X-ray, SXR and EUV radiation have major implications for exoplanets (Scalo et al. 2007, Lammer et al. 2009). M dwarfs below 0.35 solar masses are completely convective and produce a non-sun-like magnetic field (Morin et al. 2010).

Recent discoveries of magnetically active M dwarfs with very short rotation periods surprised the scientists. The strongest magnetic field known to date was found in a M dwarf. It is 7300 G and is generated by WX UMa (Shulyak et al., 2017). This magnetically very active star is an ideal example to simulate the development of induction heating in a model. For the computation, an Earth-like planet orbits WX UMa with various eccentricities within the habitable zone. In order to be able to compare the resulting results, calculations were also made for the TRAPPIST-1 system. The M dwarf TRAPPIST-1 generates a 600 G magnetic field and hosts seven exoplanets with small orbits (Reiners & Basri 2010, Gillon 2016 & 2017).

Kislyakova et al. (2017, 2018) has considered induction heating of planets orbiting on circular orbits, while your work is dedicated to induction heating of planets on eccentric orbits - an effect which has never before been considered for exoplanets orbiting M dwarfs.

1. State of the art

1. 1. Magnetic fields of M dwarfs

M dwarfs have masses of 0.1 to 0.5 solar masses and represent the largest population of stars in our galaxy (Reiners 2012). According to the results of the spectroscopic observations and the analysis of photometric light curves of 238 M dwarfs in the solar environment in the course of the MEarth exoplanet transit survey, the rotation period, the stellar age, the generation of a magnetic field and subsequent heating are closely related (Nutzman & Charbonneau 2008, Irwin et al. 2009b & 2011b, Berta et al. 2012, West et a. 2015). The star activity increases with increasing rotation speed. The loss of angular momentum caused bye magnetized winds slows the star's rotation (Skumanich 1972, Barry 1988, Soderblom et al. 1991, Barnes 2003, Pizzolato et al. 2003). The stellar activity of M dwarfs is therefore related to their longevity (Silvestri et al.,2005, West et al. 2008). Some of these small, faint stars produce very strong magnetic fields, flares and high X-ray fluxes. These little stars make one particularly interesting group (Reiners 2012, Shulyak et al. 2017). M dwarfs are the lowest-mass stars of the main sequence and due to their long main sequence life times are of great interest for the exploration of their evolution. Magnetic fields play a central role in the evolution of the stellar activity. Spectral observations identify magnetically active and inactive M stars via their H alpha emissions (Hilton 2011). The activity correlates with the age of the star (Silvestri et al., 2005, West et al. 2008). Early M dwarfs stay active for shorter periods of time in comparison to late M dwarfs (Hawley et al. 2014). Starspots and flares are observed more often in mid and late M dwarfs (Chabier & Baraffe 1997).

In contrast to sun-like stars, M dwarfs below 0.35 solar masses are fully convective and therefore seem to have no solar-type dynamo-generated magnetic field. The magnetic activities of these small stars can be detected directly via the Zeemann effect (unpolarised and circularly polarised line profiles) (Morin et al. 2010). The magnetic field of M dwarfs varies from a few Gauss to several Kilogauss. Scientists led by the University of Göttingen discovered magnetic fields up to 7000 gauss in the investigation of fast-rotating M stars. The previous theory of a saturated dynamo at 4kG, if the rotation rate of the star exceeds a specific limit, does not apply to these low-mass main sequence stars (Shulyak et al. 2017). The bistable dynamo models of spectroscopic and polarimetric studies states that stars with the strongest magnetic fields usually have dipole-dominated field geometries, while stars with the average fields less than 4 kG have fields mostly dominated by multipolar components (Garraffo 2015). This means that strong stellar magnetic fields have a very simple geometry dominated by a dipole character. But as soon as a star has a more complex magnetic field geometry, the strength of the field will be below 4000 gauss. Large-scale magnetic fields show a strong tendency to axisymmetric geometries with poloidal components in completely convective stars. By contrast, hotter, only partially convective M dwarfs have much more complex fields with toroidal components. In addition, there are a number of special cases that are fast rotating, fully convective, and generate complex, large-scale magnetic fields with a multipole geometry (Shulyak et al. 2017).

1.2. Stellar magnetic field variations

Already in 1919 Larmor developed first theories about the influence of electromagnetic induction on the magnetic field of the sun. Since then, there is great interest in dynamos of cool stars like the sun. The magnetic field of the sun results from an interaction of differential rotation (Ω effect) and cyclonic convection (α effect). This is called the αΩ dynamo. The omega effect describes the generation of an azimuthal (toroidal) field by shearing an existing meridional (poloidal) field. The re-generation of the latter by rotation and convection is referred to as alpha effect. Convection inside the sun is caused by the constantly occurring nucleus synthesis in its interior and the resulting heating (Field and Chaisson 2013, p. 85). The resulting plasma is set in motion by turbulent convective flows and forms the so-called convective zone. Due to the flow of the ionized gas, electric currents are generated which induce magnetic fields according to Ampere's law. Both laws are in chapter 1.3 explained in more detail. Varying magnetic fields, in turn, generate electric currents as Faraday describes in his law. Hot plasma shows many physical features known from liquids. To describe the solar dynamo, the magneto-hydrodynamic equation is used

$$\mathbf{E} = \frac{J}{\sigma} - v \times \mathbf{B} \qquad (1)$$

where the electric field is expressed by E, J describes the density of the electric current and the velocity of the plasma, or rather a liquid element thereof, is represented by v, σ expresses the plasma conductivity and B describes the resulting magnetic field (Seehafer 1996, Markey & Tayler 1973, Pneuman and Kopp 1971).

Both magnetic field arrangements are not stable. In the toroidal magnetic field configuration, the densification of magnetic field lines near the magnetic axis causes Tayler instabilities. This creates turbulent, convective movements. A poloidal field in a star costs its magnetic atmosphere energy because in the interior constantly counter-polar movements occur. In combination, this results in a magnetic field configuration that we find in solar-type stars (Field and Chaisson 2013, p. 85). Thanks to helioseismological data, it was possible for the first time a few years ago to study the internal differential rotation of the sun in more detail. It turned out that the interface between the radiative core and the convective shell plays a crucial role in dynamo processes. This thin transition layer between the differentially rotating outer, convective layer of the star and the rigidly rotating interior is called tachocline and presents the area where the Ω effect is able to amplify magnetic fields (Corbard et al. 1998, 2001, Charbonneau et al. 1999).

On stellar surfaces, magnetic activity manifests in flares, spots and other phenomena. Already Galileo has observed the spots on the sun's surface, a power generation inside the star. Today it is known that magnetic fields are stronger in these sunspots than in the surroundings and convection is suppressed in that spots. The sunspots occur in varying frequency and their number fluctuates in a cycle of 11 years between a minimum and a maximum. In addition to the fluctuations in solar activity, there are also varying bursts of radiation and gas and changes in the solar wind. The solar wind emanating from the sun carries about one million tons of matter per second into space at an average speed of 500km per second. The resulting helios-

phere reaches far beyond the Earth's orbit into the interstellar medium. This solar-wind-generated sphere is criss-crossed by coronal gas streams that cause numerous collisions to produce shockwaves and high-energy particles. Pressure waves generated by flares constantly heat the heliosphere (Field and Chaisson 2013, p. 76-77, 84-86).

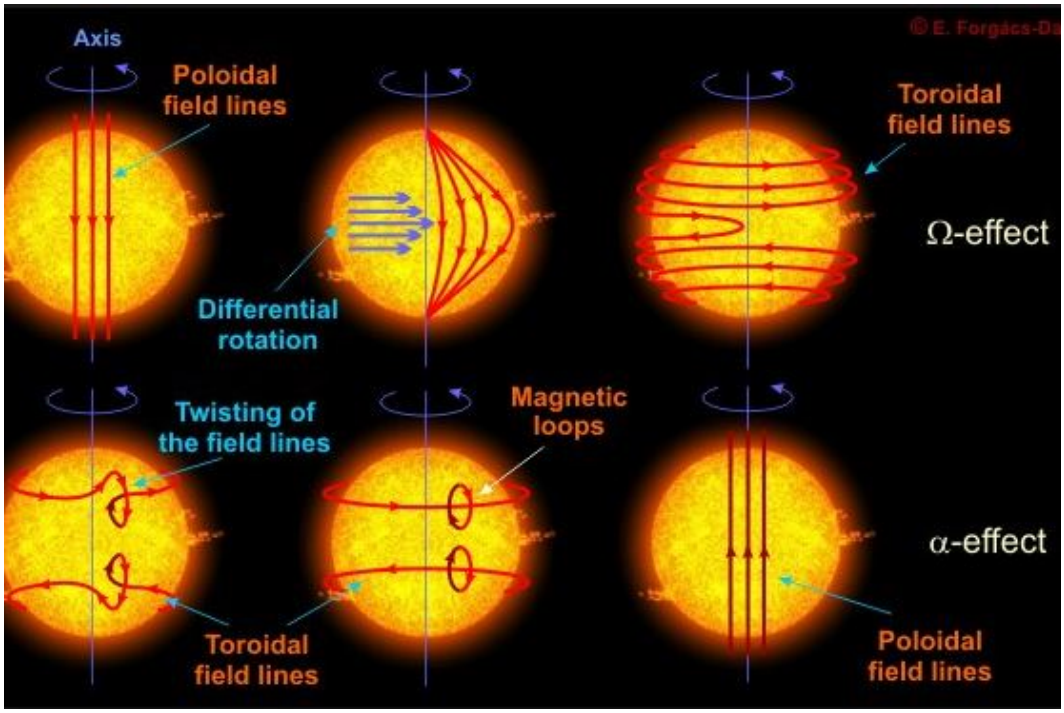

Figure 1: The Ω Effect and the α Effect. Image by E. F. Dajka (http://www.crediblehulk.org/wp-content/uploads/2017/01/alpha-and-omega.jpg)

Since cooler stars with masses below 0.35 solar masses have no tachocline, theoreticians think that cyclonic convections and turbulences have the decisive influence on their non-solar dynamo. The differential rotation of these stars has little effect on the formation of the magnetic field (Morin et al. 2010b).

Extreme stellar activities, such as coronal eruptions or flares are effects of the magnetic field. The explosive decay of magnetic fields investigated by astrophysicists as well as the reconnection of magnetic field lines pose fascinating problems in the investigation of stellar magnetic fields. Magnetic reconnection accelerates charged particles up to high energies. Reconnection of the magnetic field lines happens spontaneously and alters the magnetic field geometry. The extensive structures resulting from this interplay of decay and reconnection, which manifest as bursty eruptions, are referred to as flares. In this process, the energy of the magnetic field is transferred to the kinetic energy of charged particles, which thus become high-energy particle streams (Field and Chaisson 2013, p. 76-77, 84-86). WX UMa is a flare star and thus belongs to the class of eruptive variable stars. These small stars show and extraordinary fast and strong increase in brightness and a nearly as rapid decline to the original state (Gurzadyan 1980).

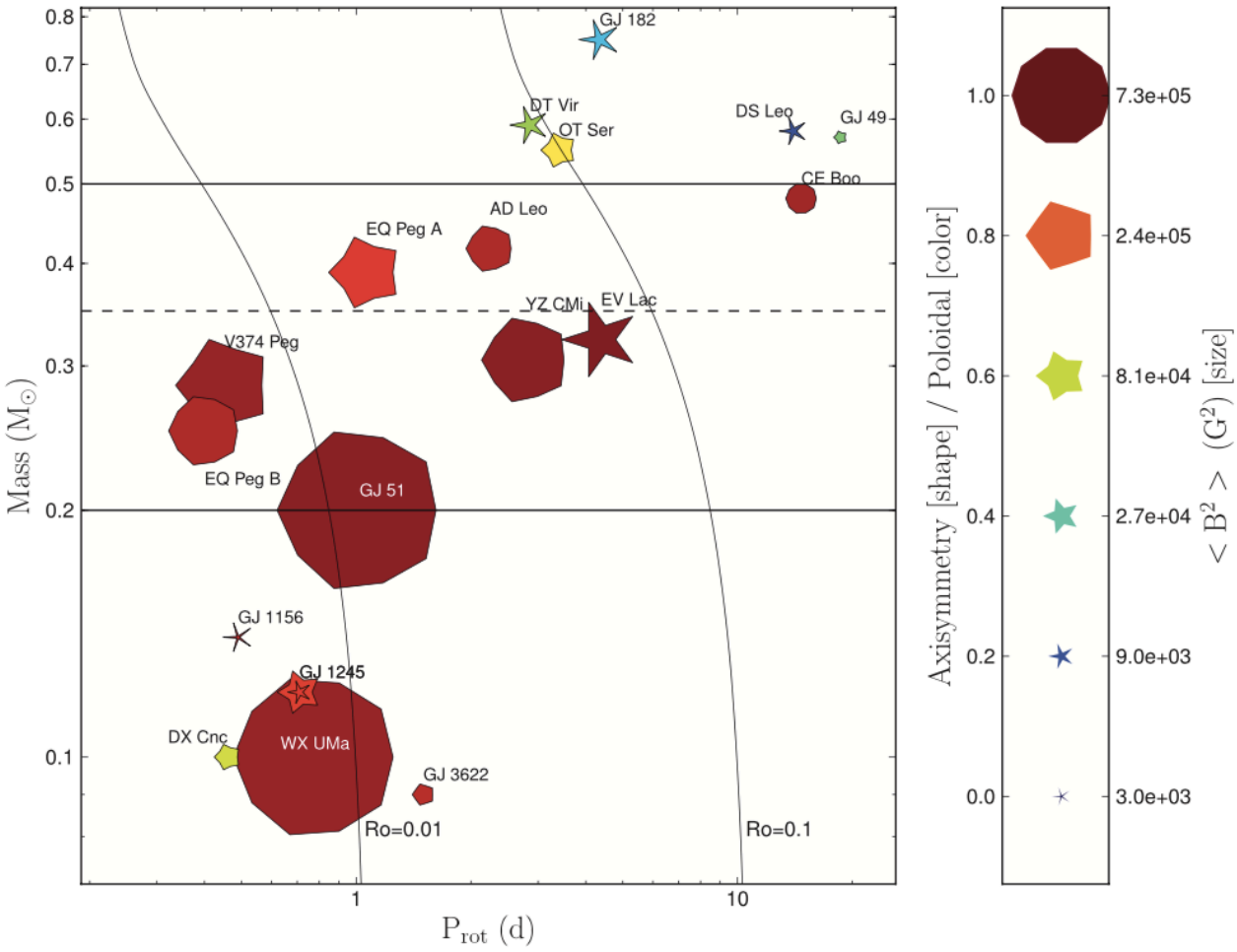

Figure 2: This plot illustrates connection between stellar masses, rotation periods, and magnetic fields.The strength of each magnetic field is represented by the size of the symbol. The axis symmetry ranges from pure axis symmetry, represented as decagons, to fully non-axis symmetry, symbolized by sharp stars. The field configurations are illustrated by purely toroidal (blue) to purely poloidal (red) by colors. The approximate saturation threshold and supersaturation threshold (solid vertical lines) corresponds to the contours of constant Rossby number Ro = 0.1, for rapidly rotating stars and Ro = 0.01 for very fast rotators (e.g., Pizzolato et al., 2003). Likewise, the simulations of Yadev et al 2016 give reason to believe that as the Rossby number of fully convective M-dwarfs increases, a transition from poloidal, quasi-steady dipole-dominant dynamos to mixed poloidal/toroidal field configurations can be observed. The horizontal lines divide the stars into groups according to their mass and M-dwarfs have masses between 0.1 and 0.5 solar masses and the horizontal dashed line represents the theoretical full-convection limit (M⋆ ≃ 0.35 M⊙, Chabrier & Baraffe 1997) figure by Morin et al. (2010).

The global average solar dipole field is of the order of 5 G during the solar minimum. However, many late-M dwarfs show much stronger magnetic fields, which can be up to several kG. The corona and chromosphere of these stars show strong magnetic activity due to the enormous heating (Hawley et al. 1996, West et al. 2004, Reiners & Basri 2008, Berger et al. 2008, Reiners & Basri 2009, Williams et al. 2014). Despite years of research, it is still not clear which mechanisms are responsible for the heating of the stellar corona and chromosphere in stars. The generation of the magnetic field and the resulting activities may be of great importance to planets orbiting M dwarfs and their habitability (Charbonneau et al. 2009, Muirhead et al. 2012, Dressing & Charbonneau 2013, 2015).

The aim of this work is to shed light on the influence of a stellar magnetic field generating electromagnetic induction heating in the mantle of an orbiting planet. In particular, the electrical currents caused by changing magnetic fluxes are the center of this investigation. There are several reasons why a stellar magnetic field acting on a planet can vary (Schwartz, Sonett, Colburn 1969). If, for example, the axis of rotation and the dipole axis deviate from one another, i.e. are not in line, these variations occur, as you can see in Figure 2a. Effects of the stellar magnetic field variability on an exoplanet shown in Fig. 2a and 2b were studied by Kislyakova et al. (2017, 2018).

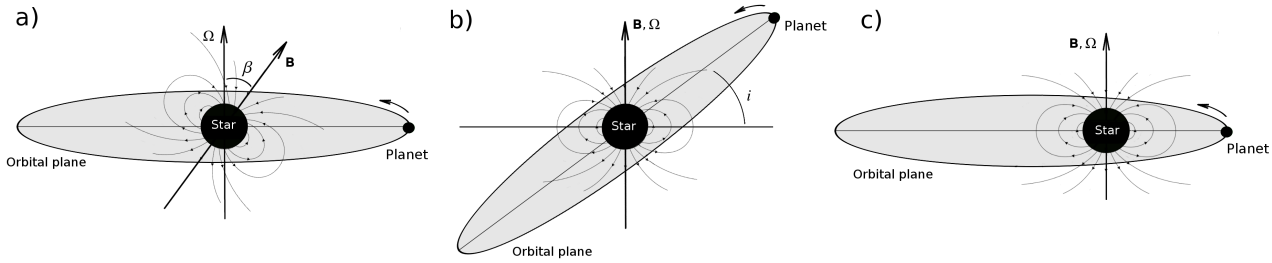

Figure 3: Varying magnetic flux densities experienced by an orbiting exoplanet. a) If the axis of rotation and the magnetic dipole axis are inclined in relation to each other, a planet with a correspondingly small distance from the star will experience a variation in magnetic flux in its interior (Kislyakova et al. 2017). b) In this model, the inclination of the orbit causes the planet to be exposed to a varying magnetic field (Kislyakova et al. 2018). c) Due to the eccentric orbit of the planet, there is a changing magnetic flux density and the associated emergence of induction heating. This creates induction heating in a),b) and c), which heats the planetary mantle mostly within an upper layer called the skin depth (figure by Kristina Kislyakova).

Another possibility for the generation of a variable stellar magnetic field surrounding the planet is an inclination of the plane of the planetary orbit to the coincident axes of the magnetic dipole and the rotation. This model is described in the work of Kislyakova et al. 2018 (Figure 2b). The current work is based on works by Kislyakova et al (2017, 2018) and considers the induction heating in rocky exoplanets with conducting mantles on eccentric orbits (Fig. 2, panel c). It can be assumed that a planet with an eccentric orbit experiences different magnetic flux densities as it moves around the star. This varying magnetic flux produces an induction voltage in the conducting planetary mantle. The aim of these model calculations is to better illustrate the dependence of the induction heating generation inside planets on the orbit's eccentricity.

1.3. Induction heating

Michael Faraday became the first to notice the effect of induction. He noted that in a conductor exposed to time-varying magnetic fields, electrical voltage is generated. He called this induction voltage, which arises if the magnetic flux is changing in time. The physical principles of induction heating can be illustrated by the help of the Maxwell equations. By combining the laws of Faraday, Ampere and Gauss and Introducing the Displacement Current, Maxwell explained the phenomena of electromagnetism with these equations and the Lorentz force (Demtröder 2006, p. 123-135). The ‚Classical Electromagnetic Theory' is completely described by

$$\vec{\nabla} \cdot \vec{\mathbf{E}} = \frac{1}{\epsilon_0}\rho_e \qquad \text{Gauss' law for E-field}$$

$$\vec{\nabla} \cdot \vec{\mathbf{B}} = 0 \qquad \text{Gauss' law for B-field}$$

$$\vec{\nabla} \times \vec{\mathbf{E}} = -\frac{\delta \vec{\mathbf{B}}}{\delta t} \qquad \text{Faraday's law}$$

$$\vec{\nabla} \cdot \vec{\mathbf{B}} = \mu_0 \vec{J}_e + \mu_0 \epsilon_0 \frac{\delta \vec{\mathbf{E}}}{\delta t} \qquad \text{Ampere's law with Maxwell's Correction} \quad (2)$$

$$\vec{F} = q_e(\vec{\mathbf{E}} + \vec{v} \times \vec{\mathbf{B}}) \qquad \text{and the Lorentz force.}$$

E stands for the field strength vector and B is the vector for the magnetic flux density. Here, μ stands for the magnetic permeability constant, it is also called the induction constant. The parameters q and ρ stand for the electric charge and the charge density. J stands for the electrical current density and ϵ_0 describes the electric field constant (Demtröder 2006, p. 123-135). Gauss's Law for electric fields describes that the presence of a charge gives rise to an E-field whose field lines have a diverging character. The absence of a magnetic monopole and the source-free field, i.e. a conservative flux, are described by Gauss's law for B fields. The law of induction, also called Faraday's law, reflects the generation of electric vortex fields (‚Wirbelfelder') by the variation of the magnetic fields. The formation of magnetic vortex fields due to electrical currents and alternating currents is described by Amperes law with Maxwell correction. In an E or B field, a force acts on each charge described by the Lorentz force. When rapidly varying magnetic fields penetrate an electrically conductive body, electrical currents are generated in the conductor called eddy currents. These heat the material by Joule heating. If the magnetic field is strong enough and the field is varying periodically, it can lead to extreme heating. Likewise non-metals can experience this effect, but with a lower yield of eddy currents. Even if the magnetic field is uniform, the eddy currents in the body are never evenly distributed. The currents concentrate towards the surface. This mechanism is called skin effect (Rudnev 2003). For a planet or moon, this means that this heating affects an outer layer of the body called the skin depth.

In our solar system, the induction heating mechanism doesn't play an important role for planets because the solar magnetic field is too weak and the planets are orbiting too far from the Sun for the effect to be substantial (DellaGuistina 2017). An exception are Jupiter's moons Io and Europe. The detection of radio emissions decades ago showed that Io is electrodynamically linked to Jupiter via a flux tube. Io feeds Jupiter's spacious magnetosphere with heavy ions that affect it dynamically and energetically. This mechanism is called the unipolar inductor (Goldreich & Lynden-Bell 1969, Spencer et al. 2000). Io moves on a nearly circular orbit that is about 90 degrees to Jupiter's axis of rotation (Stebbins and Jacobsen 1928, Harris 1961). The rotation and dipole axes of Jupiter are inclined at approximately 10 degrees to each other, so Io experiences a nearly constant magnetic field of Jupiter (Berge 1965, 1966). The flux tube of plasma between Io and Jupiter is fed from the volcanic activity of the moon. The unipolar conductor describes a conductor moving in a constant magnetic field. Io and the flux tube rotate, creating a heating of the active Jovian moon. In contrast to the unipolar conductor heating of the Io-Jupiter system (Goldreich & Lynden-Bell 1969), my model describes the induction heating of a planetary mantle that experiences, on an eccentric orbit, a varying magnetic field of the host star.

Additionally Jupiter generates an enormous amount of warming in Io due to tidal heating. A small proportion of the heating of Io is attributed to electromagnetic heating (Colburn 1980). Both results in intense volcanic activity on the surface of this moon (Goldreich & Lynden-Bell 1969). The size and strength of this magnetosphere is explained by the rapid rotation of Jupiter. In contrast, the energy for the magnetic field of the Earth is basically obtained from the solar wind (Spencer & Schneider 1996).

In the mid-1990s, the Galileo spacecraft broadcasted Radio-Doppler data from the observations of Jupiter's moon, Europa. The data showed that the interior of the moon is most likely to divide into an interior metallic core, a rocky mantle, and a nearly 80 to 170 km thick liquid shell below the ice surface (Anderson et al. 1998). More detailed data on the inner nature and interactions of Europa was provided by a 3D model of Schilling et al. (2007). The study investigated the time-dependent plasma interactions of the atmosphere and the ocean below the surface of the jovian moon. For this purpose, the time-dependent induced magnetic fields were added to older models with the plasma interaction of the atmosphere and the electromagnetic induction processes in Europa. This made it possible to determine the induced magnetic field of Europa and thus to draw conclusions about the conductivity of the ocean. Since the electrical conductivity as well as the exact thickness of the ocean determine the strength of the induced magnetic field, only statements could be made depending on different ocean depths (Schilling et al. 2007, Khurana et al. 2009).

There are some stars whose strong varying magnetic fields can produce induction heating on planets orbiting close to their host stars. In the TRAPPIST-1 system, this effect occurs (Kislyakova et al. 2017)

1.4. TRAPPIST-1 System

In 2016, the small planets around the M dwarf star TRAPPIST-1 were discovered with the South Telescope at La Silla Observatory. The orbits of the recently discovered rocky exoplanets of this nearby system are very close to the star. The dwarf star TRAPPIST-1 is located only 12 pc away from Earth and is composed of TRAPPIST-1, an M8 dwarf star and at least seven exoplanets, TRAPPIST-1b, 1c, 1d, 1e, 1f, 1g and 1h with Earth-like sizes (Gillon et al. 2016 & 2017). TRAPPIST-1, also known as 2MASS J23062928-0502285 (Gizis et al. 2000), is an ultracool dwarf star with an equilibrium temperature of 2511 ± 37 K (Delrez et al. 2018) and with an age of about 7.6 ± 2.2 Gyr and a metallicity of [Fe / H] ≈ +0.06. Its radius corresponds to R = 0.121 ± 0.003 R⊙ (Gizis et al. 2000, Burgasser & Mamajek 2017). This star is a fast rotator with a rotation period of 3.3 days (Luger et al. 2017).

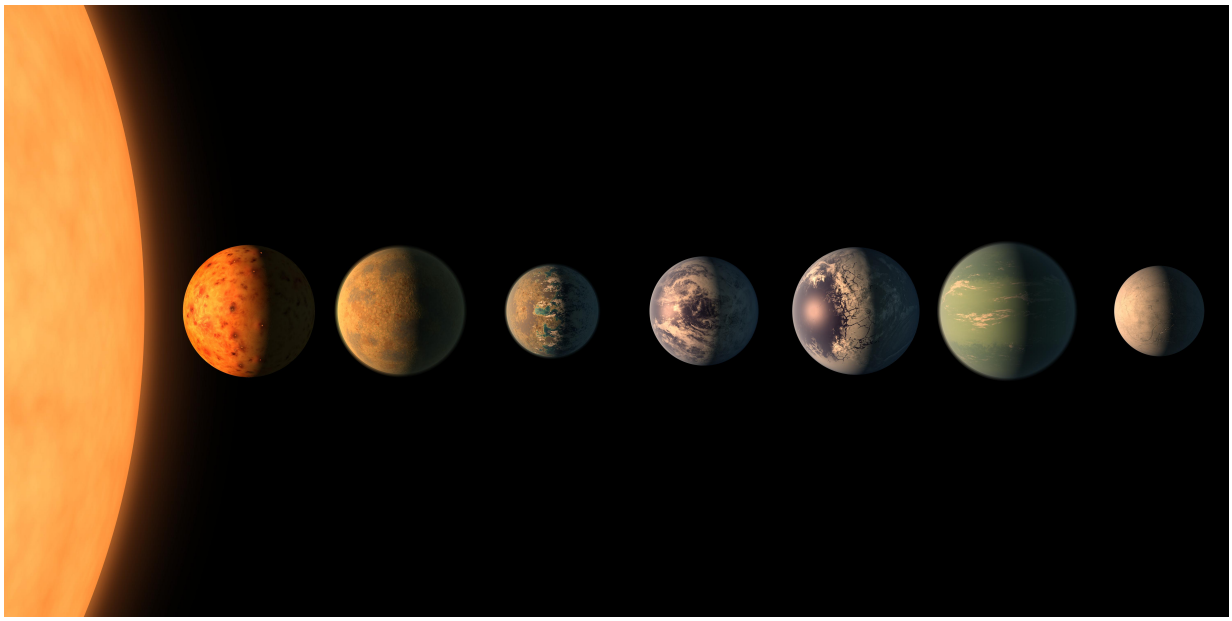

Figure 4: Artist's impression of the seven rocky exoplanets TRAPPIST 1b-1h, Image credit: NASA/JPL-Caltech

The star has a system of seven known planets forming a resonant chain (Luger et al.2017). Three of the seven planets are located in the habitable zone (Gillon et al 2017). The transit observations, which were ground-based and space-based, allowed to measure the orbital periods between 1.5 days for the innermost exoplanet and almost 19 days for TRAPPIST-1h (Burgasser & Mamajek 2017). Likewise, transmission spectroscopy gives the opportunity to make assumptions about the composition of the atmosphere of the individual planets. Combined with the radius of the dwarf star, the sizes of the planets could be determined. Knowing the mass and the density a probable composition can be assumed. Figure 1 shows the seven rocky exoplanets of the 40 light-years distant system. Due to their mass, density, radius and surface gravity, the planets around TRAPPIST-1 are very similar to Earth. However, the distances to the star as well as the orbital periods of the two systems are very different. Due to the different luminosity of the central stars, the habitable zone is 1 AU in the solar system and about 0.02-0.03 AU in the TRAPPIST-1 system. Mass and density calculations confirmed that TRAPPIST 1c and 1e mostly have rocky interiors, but planets 1b, 1d, 1f, 1g, and 1h have a high proportion of volatiles in their composition. These may be present in the form of planetary atmospheres, oceans or ice sheets. TRAPPIST-1b could potentially have water vapour of

about 10-10000 bar and is the only one of the seven planets above the runaway greenhouse limit (Grimm et al. 2018). Due to the short distance to this active M8 star, the strong energetic, stellar winds affect the surface and atmosphere of the exoplanets more intensely than on the Earth (Garraffo et al. 2016). The erosive effect of the stellar wind and the measured extreme ultraviolet plus X-ray (EUV and XUV) radiation suggest that TRAPPIST-1b and 1c could have lost oceans of water (Bolmont et al 2017). The spectral range of XUV is between 10 nm and 121 nm (ISO 21348 2007). A lower loss rate is to be expected at the third planet. According to climate models, the exoplanet TRAPPIST-1e potentially has the best conditions for the presence of liquid water on its surface (Wolf 2017). Whether and how much water these planets are able to retain depends on the original amount of water and the activity of the star (Garraffo et al. 2017). The cause of these strong XUV emissions and stellar winds are the stellar magnetic activities. TRAPPIST-1 has a short rotation period of 3.3 days (Luger et al. 2017).

The strength of TRAPPIST-1's average magnetic field has been measured to equal 600 Gauss (Reiners & Basri 2010). As already mentioned in chapter 1.3, it can come to the induction heating by the influence of strong, variable magnetic fields. This could be the case for several TRAPPIST-1 planets. Despite their location in the habitable zone, they could be uninhabitable as their surface temperatures and prevailing climate are influenced by volcanic activity and CO2 outgassing from the interior (Grimm et al. 2018, Kislyakova et al. 2017). The strong magnetic field of TRAPPIST-1 makes it an interesting target to study the induction heating in exoplanets (Reiners & Basri 2010). The aim of this work is to investigate the effects of induction heating to which this potentially Earth-like planets are exposed. We assume that the variation of the magnetic field along the planets' orbits arises due to their eccentric motion (Figure 3 panel c). The exoplanets orbit TRAPPIST-1 on orbits with very low eccentricities (see table 1). In contrast to the model of Kislyakova et al. In 2017, when the formation of induction heating was analyzed by tilted rotation and dipole axes of TRAPPIST-1, I assume a co-aligned dipole and rotation axis. In my model, the induction heating in the planetary mantle is investigated by the influence of the eccentricity of the equitorial planetary orbit, which exposes the planet to a varying stellar magnetic field.

I assume a pure dipole field for TRAPPIST-1 in my model. This assumption is justified because stars with small masses and strong magnetic fields usually have dipole-dominated magnetic fields. According to the hydrodynamic model for stars, there is an increase of turbulent diffusivities as the star radius increases. Accordingly, the increase of the stellar radius leads to a weaker dynamo action of the star (Shulyak et al. 2015). Strong magnetic fields are dominated by dipole geometries (Shulyak et al. 2017).

1.5. WX UMa

The flare star WX UMa, also called Gliese 412B, is part of the double system WDS 11055 + 4332. This M6 V star is located in the Ursa Major (Great Bear) constellation in the neighbourhood of the Sun with its distance of 4.8 pc (Morin et al. 2010, Pettersen 1991). WX UMa has a high potential for the effect we are examining. WX UMa is a fast rotating star and has a mass of about 0.1 solar masses and a radius of 0.12 solar radii. In this very active dwarf, the axis of rotation and the dipole axis of the magnetic field are almost on one line. Its large scale magnetic field (Morin et al., 2010) and its X-ray emission (Schmitt et al. 1995) have been the subject of research in the past. Spectral monitoring with the 2.6m Telescope of Byurakan Astrophysical Observatory on May 18, 2012 enabled the detection of a very strong flare on WX UMa. The small M dwarf was subject to an immense release of energy that made its spectrum resemble the one of an early B star in the short term. The star reached an increase of about 4.5 mag, assuming that the low-time resolution of the observation led to a lower amplitude measurement (Melikian et al. 2012). Probably the first detections of flares with 1.5 mag from WX UMa were observed by A. van Maanen with a 1939 Mount Wilson telescope (Joy 1967). Recent observations have shown that WX UMa has the strongest magnetic field ever found of a M star. The magnetic field has a dipole geometry, which is shown in Figure 5 (Morin t al. 2010) and a newly measured strength of 7.3 kG (Shulyak et al.2017). This flare star has an exceptionally short rotation period of 0.78 days, suggesting that WX UMa is likely to be of low age. It's magnetic field should therefore not lose stability for some Gys (Reiners 2012, Vidotto et al. 2014).

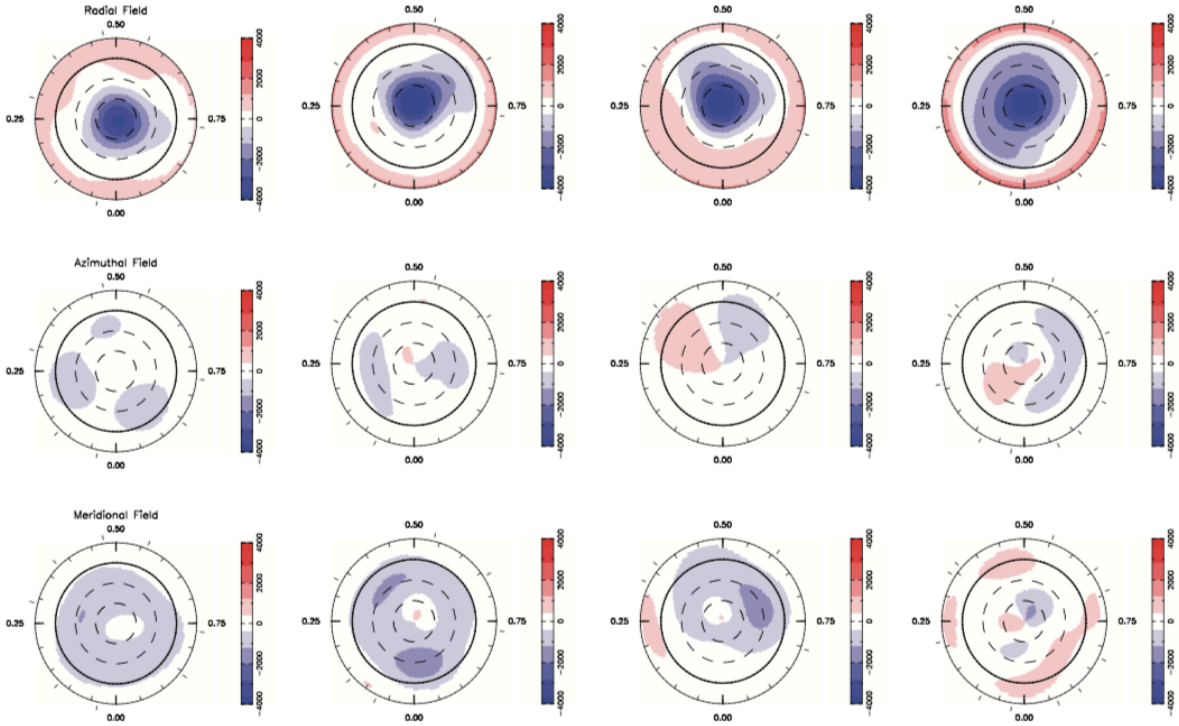

Figure 5: ZDI magnetic map of WX UMa was described by Morin et al. 2010 derived from their datasets for the years 2006 to 2009 (from left to right). The equator is illustrated with a thick circle. The flow values are shown in Gauss and the components of the field in spherical coordinates. All three are illustrated from top to bottom. The field with the negative polarity dominated the observed hemisphere at the time of observations. Here, the field lines are directed to the star and gave 2010 maximum readings of 4 kG. Both the azimuthal and the meridional field components are much weaker than the radial component of the field (figure by Morin et al. 2010)

1.6. Electrical conductivity of planetary interiors

The magnetic susceptibility (χ) describes the magnetizability (M) of matter, which is caused by H an external field χ = M / H. The Curie temperature, the temperature at which materials lose their magnetic properties, is reached in our model, at a depth of 20-90km. This means that the materials are no longer magnetic deeper than this level, and even the higher layers have the magnetic susceptibility barely different from unity. The test planet is supposed to orbit WX UMa on eccentric orbits between 0.1 and 0.9. We assume a test planet with the same mass, radius, and electrical conductivity profile as those of the Earth. The mantle rocks in the upper mantle may contain portions of para-, dia- and ferromagnetic minerals (Ferré, E. C. et al. 2014, Günther 2003).

Diamagnetic minerals have only compensated magnetic moments. The magnetic moment and the induced magnetic field point in the same direction antiparallel to the direction of the external magnetic field. The magnetic susceptability of such materials is negative. Diamagnetism can be found in almost all objects. The stronger para- and ferromagnetic effects that can be induced in rocks cover the weak diamagnetic phenomena in most cases.

If a material has a permanent magnetic moment, it is called paramagnetic. The induced magnetic moments and field point in the same direction, as well as the external magnetic field. The magnetic susceptibility is positive. The induced magnetization depends on the content of paramagnetic ions, such as doubly ionized iron, chromium or manganese.

Ferromagnetism occurs only in the metals iron, nickel, cobalt and artificial garnets (Soffel 1991). Due to the strong interactions of adjacent dipoles in a ferromagnetic metal, no external field is necessary to align its magnetic moments in small spatial areas (spontaneous magnetization) (Tipler 2004, Tauxe 2005). Each of these areas, also known as Weiß'sche districts or domains, has uniform and equal amounts of magnetic moments, but pointing in different directions. When an external magnetic field acts on the ferromagnetic metal, domains and their moments they start to be aligned, so that a preferred direction of magnetization arises. This ferromagnetic phenomenon is called a Bloch wall shift. A larger effect occurs with a stronger external magnetic field.

The so-called Barkhausen jumps describe a change in the magnetization direction within the Weiß'schen district and a strong increase in the magnetic moment. The magnetization of ferromagnetic materials is temperature-dependent. Above the Curie temperature ferromagnets behave like paramagnetic materials. The phenomenon of ferromagnetism is not linearly dependent on the field strength. It can be represented by the magnetization or hysteresis curve. Ferromagnetic materials have a very high magnetic susceptibility and a very strong induced magnetic field (Soffel 1991, Günther 2003).

Plagioclase, diopsides and enstatites are among the diamagnetic minerals. The group of paramagnetic rocks includes olivine, fayalite and serpentine. The greatest diversity is found in the ferromagnetic materials. They include chromite, manetite, titanomagnetite, pyrrhotite, maghemite, native iron, josephinite and wairauite (Ferré, E. C. et al. 2014).

The electrical conductivities of exoplanets are unknown as only approximate data for their masses and compositions are available.Therefore, in our model we assume an internal structure and an Earth-specific conductivity profile. Thus, interior profiles of exoplanets with a dry silicate mantle with low iron content (Xu, Shankland & Poe 2000, Morin et al. 2010, Yoshino et al., 2008, Yoshino & Katsura 2013) has been developed with the numerical code CHIC (Coupling Habitability, Interior and Crust). With the help of this code it is possible to calculate density profiles for exoplanets and moons. In the CHIC code, the study of habitability-relevant and feedback processes was realized by coupling different calculation models. 1D-3D models for the silicate or ice layer are available in this code. The thermochemical simulations include the temperatures of all layers, from the core of the planet to possible oceans and atmospheres (Noack, Rivoldini & Van Hoolst 2016).

To investigate the electrical conductivity (σ), the calculations on geomagnetism (Parkinson 1983) and its further application to close-in exoplanets of Kislyakova et al. 2017 serve as a basis.

$$\sigma = \sigma_0 exp\left(-\frac{\Delta H}{k_B T}\right) \quad (3)$$

In the equation for the electrical conductivity, the local temperature is expressed by T, the Boltzman constant by k_B, ΔH describes the difference of the magnetic flux density, σ_0 and ΔH vary with the mineral phase. Values for this were taken from laboratory-based studies on the conductivity in the Earth's mantle. Transition zones between the layers of the interior and the influence of different minerals in the mantle were considered in these studies (Xu, Shankland & Poe 2000, Morin et al. 2010, Yoshino et al. 2008, Yoshino, T. & Katsura 2013). For the calculations of the induction heating, the assumed 35 wt-% terrestrial iron mass fraction was settled in the core. Since the conductivity depends on the mineral phase in the mantle, my calculations refer to an Earth-like mantle. For the test planet orbiting WX UMa in the simulation, a value of $5x10^{10}$ CGS (≈5.6 Smm^{-1}) was assumed (Gaillard & Iacono Marziano 2005).

Figures 6 and 7 graphically show the conductivity profiles of the seven exoplanets in the TRAPPIST-1 system and the Earth. Following the models of Kislyakova et al in 2017 and 2018, the same profiles were used for these calculations. We assume that our test planet orbits WX UMa at a semi-major axis of 0.05 au with different eccentricities. We assume that this planet has a radius, mass, and a conductivity profile equal to that of the Earth (Figure 7).

In figure 6, R_{pl} is given in radii units of each planet and is used to determine the distance to the centre of the planet. The changes in the conductivity result from different phases in the planetary mantle. S m^{-1} serves as a unit to show the conductivity in the planetary mantle and can be converted to a CGS unit with 1.11265×10^{-10} S m^{-1}

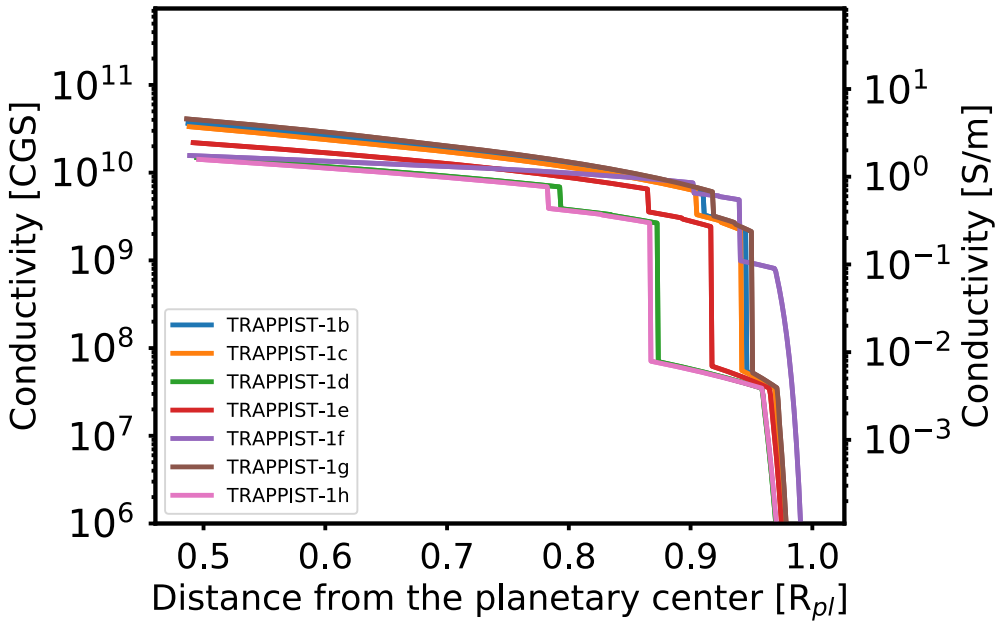

Figure 6: Conductivity profiles of the seven exoplanets in the TRAPPIST-1 system.

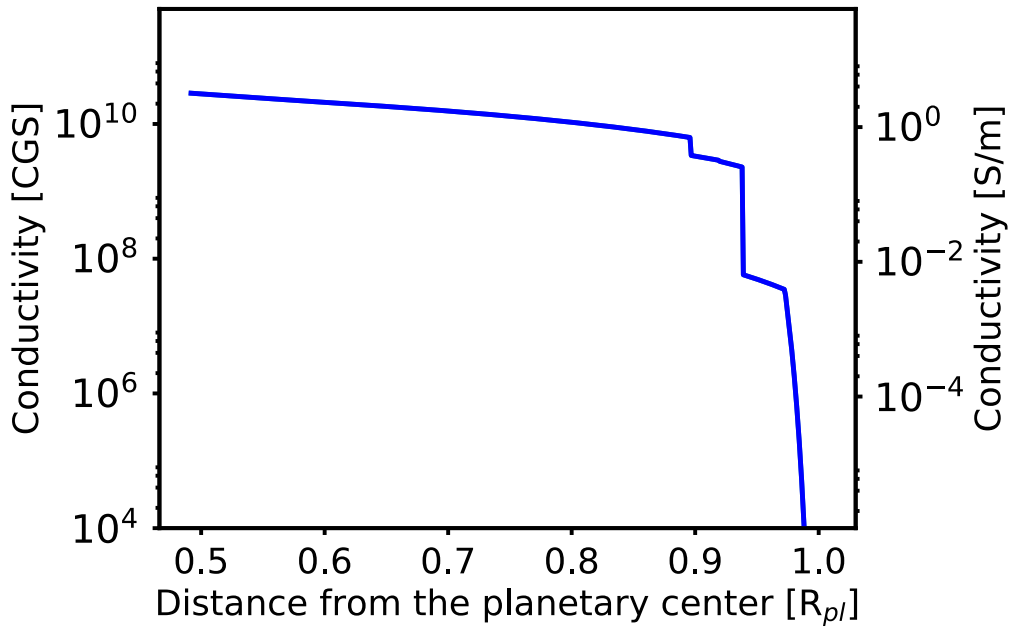

Figure 7: Earth's conductivity profile (Yoshino et al. 2008, Yoshino & Katsura 2013, and Xu et al. 2000) is the default for the calculations of the test planets orbiting WX UMa in our model. Eccentricities between 0.1 and 0.9, and a semi-major axis of 0.05 AU were set for the habitable zone for the WX UMa system.

2. Methods

The structure and composition of the planet also determines its conductivity and density profile. Whether and how much induction heating occurs in the mantle of a planet depends on the electrical conductivity and the presence of a variable magnetic field. The varying electromagnetic field doesn't freely penetrate conducting bodies, because it generates currents in the upper layer called the skin depth. The currents, in their turn, dissipate inside the body and heat it. Since the penetration depth of the external electromagnetic field is determined by the skin depth, it also determines the location of the maximum of the energy release. The skin depth and can be described by

$$\delta = \frac{c}{2\pi\sigma\mu\omega} \qquad (4)$$

The speed of light is expressed by c and σ denotes the electrical conductivity. The magnetic permeability, μ for our model as well as the permittivity (ε) μ = ε = 1. The frequency with which the magnetic filed varies is denoted by ω. For a smaller skin depth, the maximum energy release occurs closer to the surface, while for a larger skin depth, the location of the maximum is shifted deeper into the mantle (Rudnev 2003). The magnetic conductivity μ can be represented by

$$\mathbf{H} = \frac{\mathbf{B}}{\mu}$$

For the calculations $\mu = 1$ is set. This results from the consideration that the magnetic susceptibility (χ) for the density of the upper mantle corresponds to approximately 10^{-4} to 10^{-3} and therefore $\mu = 1 + \chi \approx 1$ (Belley et al. 2009). Therefore, one can assume

$$\mathbf{H} = \mathbf{B} \qquad (5)$$

Figures 8 and 9 show the density profiles and pressure profiles of the planets in the TRAPPIST-1 system and the Earth. In our model these profiles do not evolve with time as the melt fraction increases (Yoshino et al. 2006, Yoshino et al. 2010, Gaillard & Iacono Marziano 2005, Maumus et al. 2005).

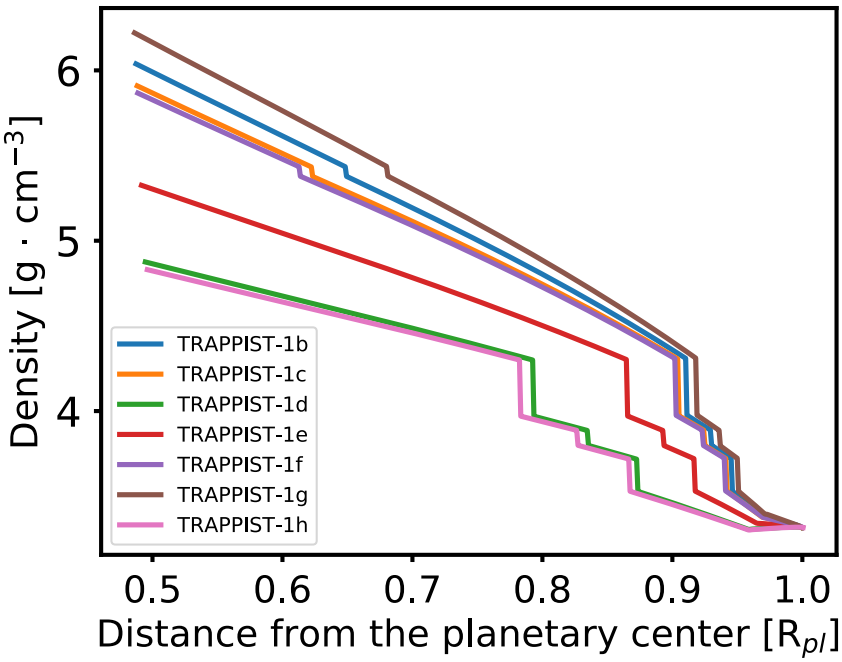

Figure 8: Density profiles of the planets in the TRAPPIST-1 system. The interior profiles of exoplanets with a dry silicate mantle with low iron content were made by using the CHIC code (Noack, Rivoldini & Van Hoolst 2015 & 2016).

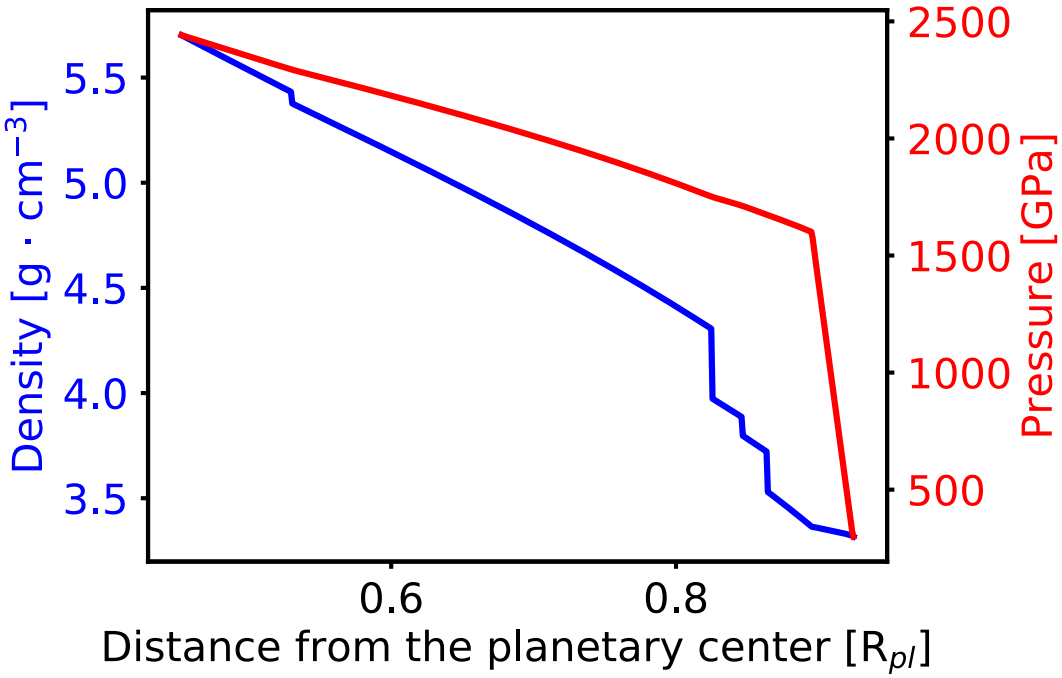

Figure 9: The density profile (in blue) and pressure profile (in red) of the Earth are the default for the calculations of the test planet that orbits WX UMa in this model. The interior profiles of exoplanets with a dry silicate mantle with low iron content were made by using the CHIC code (Noack, Rivoldini & Van Hoolst 2015 & 2016).

The magnetic field can be represented by the Maxwell equations like this:

$$\nabla^2 \mathbf{B} = \frac{4\pi\sigma\mu}{c^2}\frac{\delta \mathbf{B}}{\delta t} + \frac{\epsilon\mu}{c^2}\frac{\delta^2 \mathbf{B}}{\delta t^2}$$

If the condition $4\pi\sigma \gg \epsilon\omega$ is fulfilled, the skin effect approximation (chapter 1.3) is applicable, and the equation for the magnetic field can be written as:

$$\nabla^2 \mathbf{B} = \frac{4\pi\sigma\mu}{c^2}\frac{\delta \mathbf{B}}{\delta t} = k^2 \mathbf{B}$$

Some simplifications were necessary to be able to analytically estimate the magnitude of induction heating when a planet is exposed to a magnetic field B in its environment. B_e is the external magnetic field to which the planet is exposed on its orbit and since B = H, H_e is correspondingly the dipole field strength acting on the celestial body in its orbit. The frequency with which the magnetic field varies is represented by ω. Since $H = H_e e^{-i\omega t}$ and $B = B_e e^{-i\omega t}$, k^2 can be expressed as

$$k^2 = -\frac{4\pi i\omega\mu\sigma}{c^2}$$

Accordingly, one can represent the vector potential $\mathbf{A}$ by $\mathbf{B} = \nabla \times \mathbf{A}$ and $\nabla^2 \mathbf{A} = k^2 \mathbf{A}$. The magnetic field in spherical coordinates is described as follows (Srivastava 1966, Parkinson 1983):

$$B_r = -\left(\frac{F(r)}{r}\right) n(n+1) S_n^m$$

$$B_\theta = -\frac{1}{r}\frac{d(rF(r))}{dr}\frac{\delta S_n^m}{\delta\theta} \qquad (8)$$

$$B_\phi = -(r sin\theta)^{-1}\frac{d(rF(r))}{dr}\frac{\delta S_n^m}{\delta\phi}$$

The term $e^{-i\omega t}$ was omitted here. The function F (r) depends only on the radius. In case of a nonuniform conductivity of the upper planetary mantle $k^2 \neq$ constant. For the individual layers of the spectrum, however, a homogeneous conductivity is assumed, thus k^2 is constant in the individual layers (Srivastava 1966, Parkinson 1983). The planet is now divided into m

layers, with the last representing the core and the first the surface. Induction heating can be calculated within each layer. The potential of the external magnetic field can be described as follows

$$U_e = B_e \left(\frac{r^n}{R_{pl}^{n-1}} S_n^m(\theta, \phi) e^{-i\omega t} \right)$$

To describe the magnetic field in the jth layer, the following equations are used (Parkinson 1983)

$$B_r = (rk_j)^{-\frac{1}{2}} r^{-1} \left[C_j J_{n+\frac{1}{2}}(rk_j) + D_j J_{-n-\frac{1}{2}}(rk_j) \right] n(n+1) S_n^m$$

$$B_\theta = r^{-1} \left[C_j J^*_{n+\frac{1}{2}}(rk_j) + D_J J^*_{-n-\frac{1}{2}}(rk_j) \right] \frac{\delta S_n^m}{\delta \theta}$$

Here, J stands for the Bessel function, which is used to study the frequency spectrum of signals or other waves. It is of the first genus and the derivative of the Bessel functions is given by

$$J^*_m(rk_j) = \frac{d}{dr} \left[\left(\frac{r}{k_j} \right)^{\frac{1}{2}} J_m(rk_j) \right] \qquad (9)$$

The derivatives can be written as follows:

$$J^*_{n+\frac{1}{2}}(rk_j) = (rk_j)^{\frac{1}{2}} J_{n-\frac{1}{2}}(rk_j) - n(rk_j)^{-\frac{1}{2}} J_{n+\frac{1}{2}}(rk_j)$$

$$J^*_{-n-\frac{1}{2}}(rk_j) = -(rk_j)^{\frac{1}{2}} J_{-n+\frac{1}{2}}(rk_j) - n(rk_j)^{-\frac{1}{2}} J_{-n-\frac{1}{2}}(rk_j)$$

Using the equation for the magnetic field within the sphere, F (r) can be represented as follows:

$$F(r_j) = C_j(rk_j)^{\frac{1}{2}}J_{n+\frac{1}{2}}(rk_j) + D_J(rk_j)^{\frac{1}{2}}J_{-n-\frac{1}{2}}(rk_j) \qquad (10)$$

Assuming a homogeneous external magnetic field, one gets $n = 1$ and $cos\theta$ for the surface spherical harmonics. In this case U_e corresponds to $B_e rS_1(\theta, \varphi)e^{-i\omega t}$. Which in turn equals with $B_e r \cos\theta\, e^{-i\omega t}$. Within the sphere $B\varphi = 0$. Thus, only one φ-component remains in the vector potential and has this form:

$$A_\phi = F(r)sin\theta e^{-i\omega t}$$

By the following equation, the two previously mentioned constants Cj and Dj are interlinked with each other:

$$C_J\alpha_j = C_{J+1}\beta_j + D_{J+1}\gamma_j$$

$$D_J\alpha_j = C_{J+1}\delta_j + D_{J+1}\epsilon_j$$

and

$$\alpha_j = J^*_{-n-\frac{1}{2}}(r_jk_j)J_{n+\frac{1}{2}}(r_jk_j) - J_{-n-\frac{1}{2}}(r_jk_j)J^*_{n+\frac{1}{2}}(r_jk_j) \qquad (10)$$

$$\beta_j = \left(\frac{k_j}{k_{j+1}}\right)^{\frac{1}{2}} J_{n+\frac{1}{2}}(r_jk_{j+1})J^*_{-n-\frac{1}{2}}(r_jk_j) - J^*_{n+\frac{1}{2}}(r_jk_{j+1})J_{-n-\frac{1}{2}}(r_Jk_J)$$

$$\gamma_j = \left(\frac{k_j}{k_{j+1}}\right)^{\frac{1}{2}} J_{-n-\frac{1}{2}}\left(\frac{k_j}{k_{j+1}}\right)J^*_{-n-\frac{1}{2}}\left(\frac{k_j}{k_j}\right) - J^*_{-n-\frac{1}{2}}\left(\frac{k_j}{k_{j+1}}\right)J_{-n-\frac{1}{2}}\left(\frac{k_j}{k_j}\right)$$

$$\delta_j = J^*_{n+\frac{1}{2}}(r_Jk_{j+1})J_{n+\frac{1}{2}}(r_jk_j) - \left(\frac{k_j}{k_{j+1}}\right)^{\frac{1}{2}} J_{n+\frac{1}{2}}(r_jk_{j+1})J^*_{n+\frac{1}{2}}(r_jk_j)$$

$$\epsilon_j = J^*_{-n-\frac{1}{2}}(r_jk_{j+1})J_{n+\frac{1}{2}}(r_jk_j) - \left(\frac{k_j}{k_{j+1}}\right)^{\frac{1}{2}} J_{-n-\frac{1}{2}}(r_jk_{j+1})J^*_{n+\frac{1}{2}}(r_jk_j)$$

The recursive representation can be created with the help of the assumption that $R_j = \frac{C_j}{D_j}$.

$$R_j = \frac{R_{j+1}\beta_j + \gamma_j}{R_{j+1}\delta_j + \epsilon_j}$$

The conductivity at the core-mantle boundary corresponds in this model to the center of the sphere. Thus, in the center of the sphere $k = k_m$, where km is the conductivity of the core. If now D_m is set equal to zero, a singularity in the center of the sphere can be avoided and

$$R_{m-1} = \frac{\beta_{m-1}}{\delta_{m-1}}$$

corresponds to the starting value for the recursive equation, which represents the conditions for the first boundary condition. The ratio of the amplitudes of the external and internal magnetic fields at the surface equals

$$\frac{B_i}{B_e} = \frac{R_1\beta_0 + \gamma_0}{R_1\delta_0 + \epsilon_0} \qquad (11)$$

However, this ratio can only be expected on the surface of the sphere, where r equals R_{pl}. The values of β_0, γ_0, δ_0 and ε_0 are expressed as follows

$$\beta_0 = n\left[(ak_1)^{\frac{1}{2}} J^*_{n+\frac{1}{2}}(ak_1) - (n+1)J_{n+\frac{1}{2}}(ak_1)\right]$$

$$\gamma_0 = n\left[(ak_1)^{\frac{1}{2}} J^*_{-n-\frac{1}{2}}(ak_1) - (n+1)J_{-n-\frac{1}{2}}(ak_1)\right]$$

$$\delta_0 = (n+1)\left[(ak_1)^{\frac{1}{2}} J^*_{n+\frac{1}{2}}(ak_1) + nJ_{n+\frac{1}{2}}(ak_1)\right]$$

$$\epsilon_0 = (n+1)\left[(ak_1)^{\frac{1}{2}} J^*_{-n-\frac{1}{2}}(ak_1) + nJ_{-n-\frac{1}{2}}(ak_1)\right]$$

The individual spherical coordinates of the magnetic field can be expressed through (Parkinson 1983)

$$B_r = -[B_e n - (n+1)B_i]S_n^m = -[B_e - 2B_i]cos\theta$$

$$B_\theta = -(B_e + B_i)\frac{\delta S_n^m}{\delta \theta} = (B_e + B_i)sin\theta$$

$$B_\phi = (B_e + B_i)(sin\theta)^{-1}\frac{\delta S_n^m}{\delta \phi} = 0$$

The resulting eddy currents of within each layer are given by

$$\nabla \times \mathbf{B} = \frac{4\pi}{c}\mathbf{j} \ . \qquad (12)$$

There $\nabla \times \mathbf{B} = \nabla^2 \mathbf{A} = k^2 \mathbf{A}$. In which A is given by $A_\phi = F(r)sin\theta e^{-i\omega t}$. By substituting k^2 the equation can be simplified to a component for the flow in the jth layer of the planetary mantle

$$J_{\phi_j} = -\frac{i\omega\mu\sigma_j}{c}F(r_j)sin\theta e^{-i\omega t}$$

Q_j represents the calculated energy release in the corresponding layer.

$$Q_j = \frac{1}{2\sigma_j}\int |j_{\phi_j}|^2 dV \qquad (13)$$

Here, ω describes the frequency of the variation of the magnetic field and equals the frequency of the planet's orbital motion

$$\omega = \omega_{pl}$$

since ω is determined by the exoplanet's eccentric orbit. The frequency of the orbital motion of the planet ω_{pl} determines the skin depth δ (equation 4), which describes the characteristically penetration depth of the electromagnetic field in the planet's mantle (described in chapter 2).

In this work, I calculate energy release which is generated due to eccentric orbital motion of a planet. I assume a dipole-dominated stellar magnetic field, and a case where the stellar rotational axis is co-aligned with the stellar dipole axis. The seven planets of TRAPPIST-1 have small eccentricities (e). Values between 0.1 and 0.9 for e and a semi-major axis (a) of 0.05AU, according to the orbital habitable zone around WX UMa were assumed for the test planets. For the calculation of average and extreme orbital values of an elliptic orbit, Kepler's second law is: "The radius vector is equally large in equal times“.

Halfway between aphel and perihel of the orbit, the largest and smallest distance to the star, the celestial body moves at a mean line speed v_m with time t and the path traveled is represented by s_m. Thus, the area of a triangle (A), which must stay constant in time, can now be calculated:

$$A = \frac{1}{2} s_m b$$

for the semi-minor axis $b = a\sqrt{1-e^2}$ is set and the double area is used for simplicity:

$$2A = s_m a\sqrt{1-e^2}$$

If one denotes the baseline of the triangle in the perihelion by S_{ph}, the height is described by the distance to the perihelion $q = a(1-e)$, then the following expression for $2A$ can be written

$$2A = s_{ph} q = s_{ph} a(1-e)$$

According to the 2nd Kepler's Law A is constant. Therefore, one can write

$$s_m a\sqrt{1-e^2} = s_{ph} a(1-e) \qquad \text{reshaped} \qquad \frac{s_{ph}}{s_m} = \frac{a\sqrt{1-e^2}}{a(1-e)}$$

Here, t is also constant and thus the relation of the paths traveled is equal to orbit velocities of the planet:

$$\frac{v_{ph}}{v_m} = \frac{s_{ph}}{s_m}$$

eliminating the semi-major axis a, we get

$$v_{ph} = v_m \frac{\sqrt{1-e^2}}{1-e}$$

The orbital speed in the aphelion v_{ah} is described by means of the apical distance $p = a(1+e)$

$$v_{ah} = v_m \frac{\sqrt{1-e^2}}{1+e}$$

If one looks at the ration of these two velocities, it becomes clear that the orbital velocity in the perihelion is greater than that in the aphelion

$$\frac{v_{ph}}{v_{ah}} = \frac{1+e}{1-e}$$

If an exoplanet has an eccentric orbit, it experiences a variation of the stellar magnetic field along its orbit. For the further calculation it is necessary to determine ΔB, which results from the maximum radial field strength (B_{max}) minus the minimum radial field strength (B_{min}) along the orbit of the planet. In this case, this means that the planet is exposed to B_{max} in the

range of its minimum distance to the star, the periapsis, and when the maximum distance to the star, the apsis, is reached, the applied magnetic field strength is expressed by B_{min}. Thus, the calculations of $Rorb_{min}$ and $Rorb_{max}$ were necessary (Broda 2007, p. 209).

$$Rorb_{min} = a(1 - e)$$

$$Rorb_{max} = a(1 + e) \qquad (14)$$

Thus one receives

$$\Delta B = B_{max} - B_{min} \qquad (15)$$

The corresponding results for orbital radii and ΔB for the exoplanets in the TRAPPIST-1 system and for the test planet of WX UMa are listed in table 1 and 2.

The magnetic field at the stellar surface of TRAPPIST-1 and WX UMa is set according to the observations. Using the potential-field-source-surface model (PFSS), the variation of the magnetic field along the planetary orbit can be calculated (Mackay 2002, Gregory & Donati 2011). In order to extrapolate stellar magnetic fields, it is not sufficient to use the general potential field extrapolation, ignoring the fact that stellar winds extend the magnetic field lines of stars in the radial direction. This effect caused by star winds can be included in the calculations using the PFSS method. (Altschuler & Newkirk 1969, Jardine et al., 1999). In the PFSS method it is assumed that the star magnetic field loses strength differently according to the distance. For distances closer than $r < R_{SS}$ the field strength decreases with r^{-3} for a dipole. A decrease in the field strength of r^{-2} is to be expected for $r > R_{SS}$ (Johnstone 2012).

Circular orbits can be described by a simple sinusoidal function with a single frequency, but in case of an eccentric motion (especially if other larger planets are present in the system), the orbital motion takes a more complex form and cannot be described by a single sine wave anymore. For this reason, we introduce a spectrum of a signal, which will allow us to determine the amplitude of separate harmonics. Then, we can calculate energy release for each one of them. The resulting signal can be converted into a continuous function by means of the Fourier Transformation (FT). In principle, the FT signals are split into several sine functions that differ in their phases, amplitudes and frequencies. Since a signal that was previously in a time domain with the Fourier transform can be converted into a frequency range, so easily changes can be made. Frequencies that are disturbing or missing can simply be supplemented, deleted or changed.

$$F(\omega) = \frac{1}{\sqrt{2\pi}} \int_{-\infty}^{\infty} f(t) e^{i\omega t} dt \qquad (16)$$

Here, $f(t)$ is a function of time, and $F(\omega)$ is its Fourier transform. The frequency spectrum can be represented by the function $F(\omega)$. For the discrete representation we have

$$F_k = \sum_{j=0}^{N-1} f_j e^{\frac{-i2\pi kj}{N}}$$

where k = 0, …, N - 1.

$$\omega = e^{-\frac{i2\pi}{N}}$$

it follows

$$F_k = \sum_{j=0}^{N-1} f_j w^{kj}$$

This is the inverse form of the Fourier Transform (IFT)

$$f_j = \frac{1}{N} \sum_{k=0}^{N-1} F_k e^{\frac{i2\pi kj}{N}}$$

Auxiliary constants for the calculations are represented by the factor N. Therefore factor 1 / N is used for the inverse Fourier transformation. The Fast Fourier Transformation (FFT) is used to efficiently calculate the FT. James Cooley and John W. Tukey simplified the analysis of data by developing the FFT algorithm (Cooley & Tukey 1965). With this algorithm, it is possible to perform faster data processing of a digital signal. The decomposition and analysis of the frequencies is significantly shortened by the use of intermediate results because it can be dispensed with multiple arithmetic operations. The Fast Fourier Transformation is the best algorithm for FT calculations. The basic requirement for N is that is has to be a multiple of 2 (Metzner & Schaal 2002).

The orbital motion curves were calculated by Mag. Dr. Elke Pilat-Lohinger by integrating the motion equations for a planet in a two-body problem assuming a semi-major axis a = 0.05 AU and the orbital eccentricities of $0.1 < e < 0.9$ (Stumpff 1959, Murray & Dermott 1999).

After calculating amplitudes and frequencies from the data of the orbital elements by means

of FFT, the energy release (Q_j) for all frequencies for the respective conductivity profile can be calculated. Beforehand, the Nyquist frequency f_c must be set. The sampling theorem states that at least two samplings per period are needed to restore a function of frequency from a function of time f_j. The Nyquist frequency is thus to be understood as the highest frequency that can be represented (Metzner & Schaal 2002).

$$f_c = \frac{1}{2t_a} \qquad (17)$$

The time step between two consecutive time values is expressed by t_a. Should a signal with frequencies higher than the Niquist frequency be analyzed by FFT, incorrect results can be achieved. The frequencies above the f_c would be reflected in the "Nyquist range" and distort the results. This error is known as aliasing (Metzner & Schaal 2002).

3. Results

All calculations and corresponding graphics were done using Python 2.7. Additional program libraries such as NumPy, SciPy and Matplotlib were used to process arrays and perform Fourier transforms and linear algebra tasks. To implement the model setup, the program designed by Kristina Kislyakova et al. 2017 and 2018 was used and modified to calculate the generation of induction heating in the mantle of exoplanets with eccentric orbits.

The test planet orbiting the star WX UMa was calculated for different eccentricities. The semi-major axis was set at 0.05 to be in the range of the habitable zone of WX UMa. In order to generate induction heating in the outer mantle of a planet, a strong magnetic field is necessary. In addition, this magnetic field must have a high frequency of variations. TRAPPIST-1 and WX UMa are active fast rotating dwarfs, that's why they are interesting targets for investigation of induction heating (Kislyakova et al. 2017 & 18, Shulyak et al. 2017). The comparison of the TRAPPIST-1 system with nearly circular planetary orbits of the seven planets and the test planets with eccentricities between $0.1 < e < 0.9$ orbiting WX UMa in this model reveals that eccentric orbits are responsible for the generation of high frequencies of magnetic field variations. In addition to the low orbital eccentricities, TRAPPIST-1 with its 600 G field has about a 12 times weaker magneto field than WX UMa (Reiners & Basri 2010, Shulyak et al. 2017).

3.1. Induction heating of the planets in the TRAPPIST-1 system

In order to objectively discuss the influence of high eccentricities on the formation of induction heating in the planetary interior in this work, it is expedient for comparison to use a system with nearly circular orbits. For the latter, the possible occurrence of this effect for the planets of TRAPPIST-1 is calculated. The magnetic field of this fast rotating M dwarf corresponds to 600 G (Reiners & Basri 2010).

TRAPPIST-1 system	M ⊕	a (AU)	e	Rorb-min (AU)	Rorb-max (AU)	ΔB (G)	Q (erg s^{-1})
b	1.32	0.012	0.006	0.012	0.012	0.006	$7.5 * 10^{17}$
c	1.19	0.016	0.007	0.016	0.016	0.004	$1.3 * 10^{17}$
d	0.40	0.022	0.008	0.022	0.0225	0.002	$9.5 * 10^{14}$
e	0.70	0.029	0.005	0.029	0.0294	0.001	$1.1 * 10^{14}$
f	1.15	0.039	0.011	0.038	0.039	0.001	$8.3 * 10^{13}$
g	1.50	0.047	0.002	0.0468	0.047	0.0001	$2.2 * 10^{12}$
h	0.38	0.060	0.006	0.0616	0.0623	0.0002	$1.1 * 10^{12}$

Table 1: Parameters and the heating rates of TRAPPIST-1 planets for calculations: Rorb-min/max describes the minimum and maximum of the orbital radius and M the mass of the exoplanet. ΔB is the difference in the magnetic field strength at the perihel and aphel of the orbit and is given in Gauss (G). The totally mantle-averaged induction heating is expressed by Q.The semi-major axis of the orbits are denoted by a, and the eccentricities by e (Grimm et al 2018).

Through the energy release, Q and the variation of the magnetic flux, ΔB, it becomes clear that even small deviations of a near-star, circular orbit cause induction heating in the planet's interior. But, due to the small distance between each other and the host star, the planets in the TRAPPIST-1 system are exposed to tidal forces. Tidal interactions can influence the evolution of the planet orbits (Ferraz-Mello et al. 2008), as demonstrated by tidal simulations of the TRAPPIST-1 system. Within a few million years, no orbit would have an eccentricity over 0.01. To achieve significant values for tidal heating, orbits with small eccentricities are suitable (Luger et al. 2017). Achieving correspondingly high results for induction heating in my model requires greater orbit eccentricities. Thus, a planetary mantle experiences a varied magnetic field in its orbital motion. The rotation and dipole axis are assumed to be co-aligned. The energy release due to induction heating (see table 1) of the individual planets is well below the internal energy release of the Earth by radioactive decay of $2.1 * 10^{20}$ erg / s (Schubert et al 2001). The main source of internal energy of these exoplanets is tidal heating. The tidal heat flux of TRAPPIST-1b, TRAPPIST-1c, TRAPPIST-1d, TRAPPIST-1e and TRAPPIST-1g each exceeds the total heat flux of Earth (Luger et al. 2017). According to Barr et al. (2018), the tidal flux simulations for the TRAPPIST-1 planets d, e and f even exceed twenty times the mean heat flux of our planet. The tidal heating of TRAPPIST-1b's mantle results in a surface heat flux of approximately 3 watts per square meter. This value equals twice the surface heat flux of Io (Spencer et al 2000, Veeder et al. 2004) and this Jupiter moon shows the strongest volcanism in the entire solar system (Schubert et al. 2004).

Energy releases and skin depts of TRAPPIST-1 planets 1b-1h

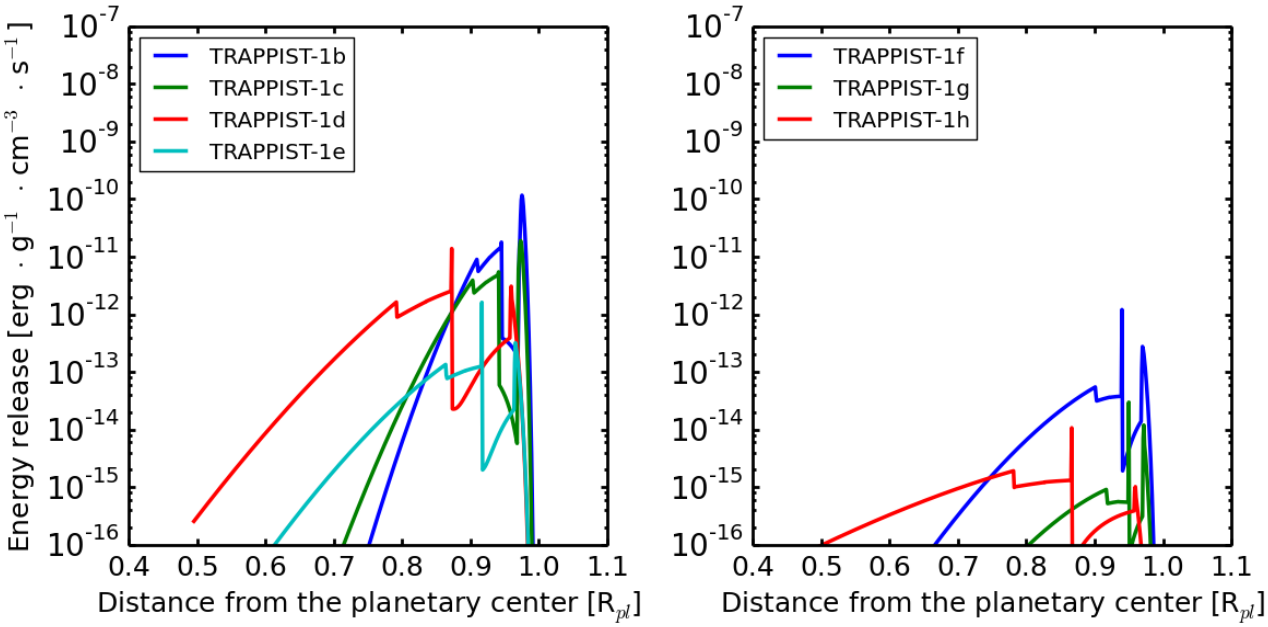

Figure 10: The energy release in planetary interiors is shown on the left for TRAPPIST-1b, TRAPPIST-1c, TRAPPIST-1d, and TRAPPIST-1e, and on the right for the three outer planets TRAPPIST-1f, TRAPPIST-1g, and TRAPPIST-1h. As a result of the increase of the semi-major axis, as shown in Table 1, the maximum energy release shifts in deeper regions of the planetary mantle and also clearly decreases in magnitude.

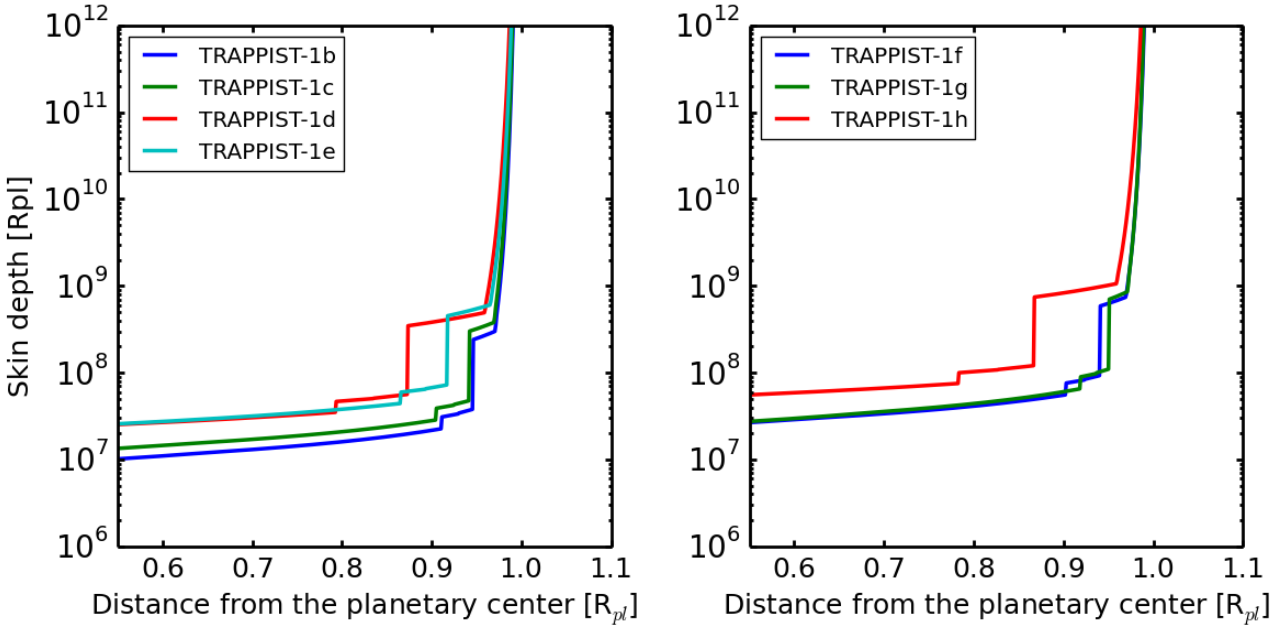

Figure 11: The Skin depth of the exoplanets of the TRAPPIST-1 System. As explained in chapter 2, the skin depth results from the skin effect, which determines that only the outer layers of the planetary mantle are affected by induction heating (Rudnev 2003).

3.2. Induction heating of a test planet orbiting WX UMa

Previously, we have studied the magnitude of induction heating on planets with small orbital eccentricities, using the seven TRAPPIST-1 planets as an example. We have shown that for small eccentricities the energy release is negligible. In this section, we study the case of higher eccentricities $0.1 < e < 0.9$ for an Earth-like test planet in the habitable zone. We choose WX UMa as a test star because of its strong observed magnetic field of 7.3 kG. The orbital motion curves have been calculated by Dr. Pilat-Lohinger (Stumpff 1959, Murray & Dermott 1999). The conductivity profile is shown in Figure 8.

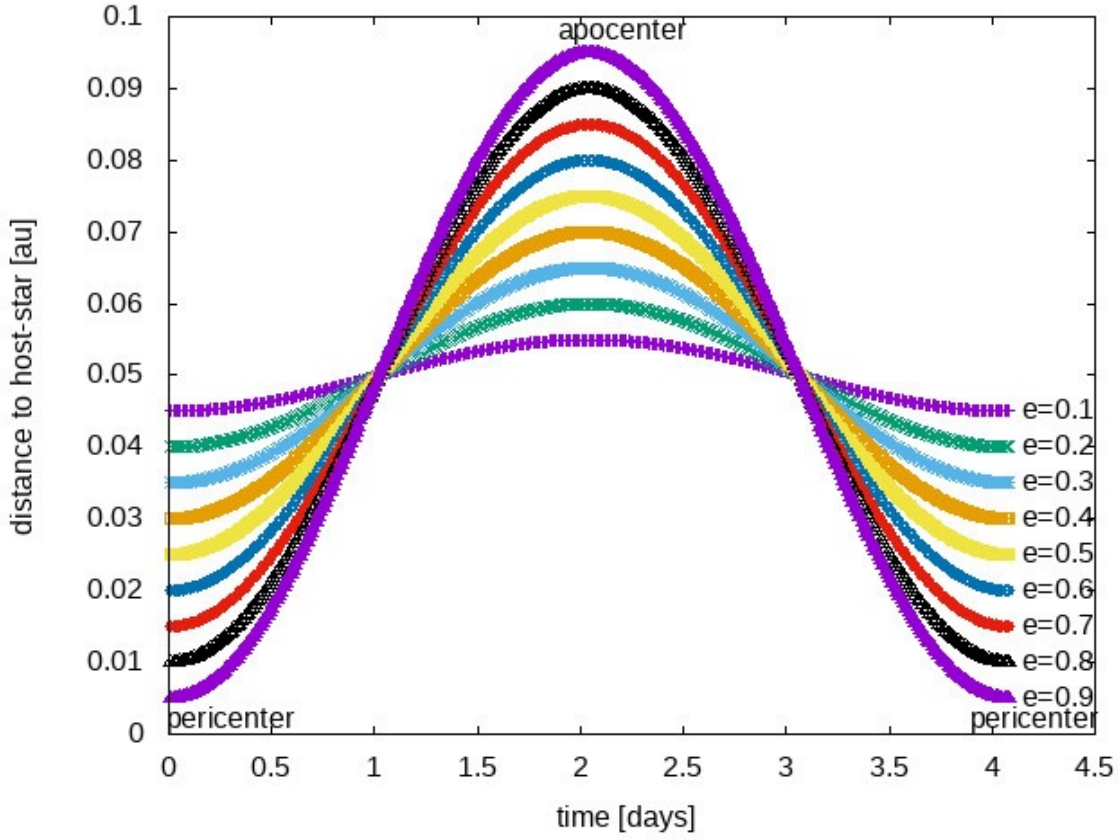

Figure 12: Various orbits were calculated for the test planet of WX UMa. The calculations were made for eccentricities between 0.1 and 0.9. The semi-major axis of 0.05 AU and a orbital period of 4.2 days were assumed. The diagram was created by Mag Dr Elke Pilat-Lohinger.

Due to its very strong magnetic field of 7,3kG (Shulyak et al. 2017), this star would have a high potential for the generation of induction heating of surrounding planets. So far, no planets orbiting WX UMa have been discovered. WX UMa is an M6 star with a mass of approximately 0.1 solar mass and a radius of 0.12 solar radii. In this very active dwarf, the axis of rotation and the dipole axis of the magnetic field are almost coaligned (Morin et al. 2010).

WX UMa test planet	a (AU)	Rorb-min (AU)	Rorb-max (AU)	ΔB (G)	Q (erg s^{-1})
e = 0.1	0.05	0.045	0.055	0.074	$3.5 * 10^{17}$
e = 0.2	0.05	0.04	0.06	0.158	$1.6 * 10^{19}$
e = 0.3	0.05	0.035	0.065	0.264	$4.4 * 10^{19}$
e = 0.4	0.05	0.03	0.07	0.412	$1.1 * 10^{20}$
e = 0.5	0.05	0.025	0.075	0.647	$2.6 * 10^{20}$
e = 0.6	0.05	0.02	0.08	1.066	$7.1 * 10^{20}$
e = 0.7	0.05	0.015	0.085	1.958	$2.4 * 10^{21}$
e = 0.8	0.05	0.01	0.09	4.49	$1.2 * 10^{22}$
e = 0.9	0.05	0.005	0.095	18.14	$2.1 * 10^{23}$

Table 2: Orbital parameters and energy release for a test planet orbiting WX UMa. Rorb-min/max describes the minimum and maximum radius of the elliptical orbit. The test planet has a mass, radius, and conductivity equal to those of the Earth.

Compared to the ΔB and Q values from the TRAPPIST-1 system, which are affected by different distances to the star and different eccentricities, the semi-major axis a for the WX UMa model was fixed at 0.05 AU. Thus, it was possible to illustrate the increase in energy release and its strong dependence on the increasing variability of magnetic flux as the orbital element of planetary orbit increases from e = 0.1 to e = 0.9. Figure 14 shows that most of the released energy is found in the mantle. Lower frequencies of the magnetic field variations have a greater depth effect. In the direction of the planetary core, the energy release decreases because of the conductivity profile, which reduces the development of induction heating. Another peak can be seen close to the surface (Ferré et al. 2014, Günther 2003).

Energy release and skin depth of WX UMa test planets

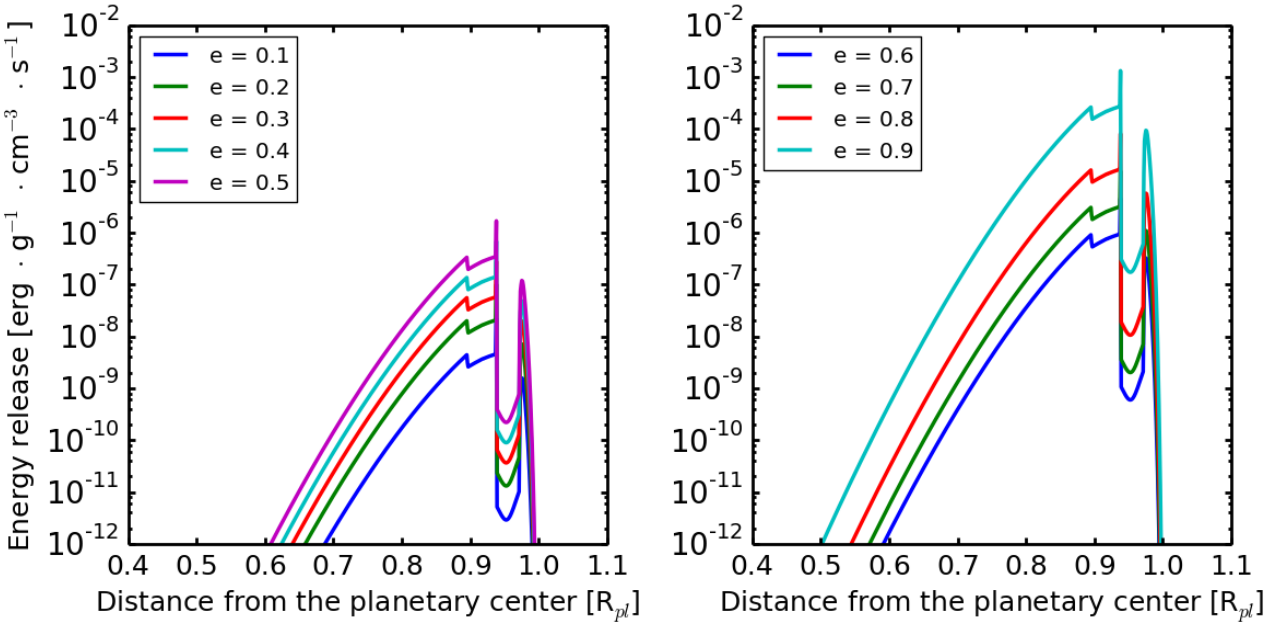

Figure 13: The distribution of the energy release inside the Earth-like planet for different eccentricities. The results as summarized for planetary orbits with 0.1 <e < 0.5 in the left image and on the right for eccentricities between 0.6 and 0.9. The semi-major axis is 0.05 AU.

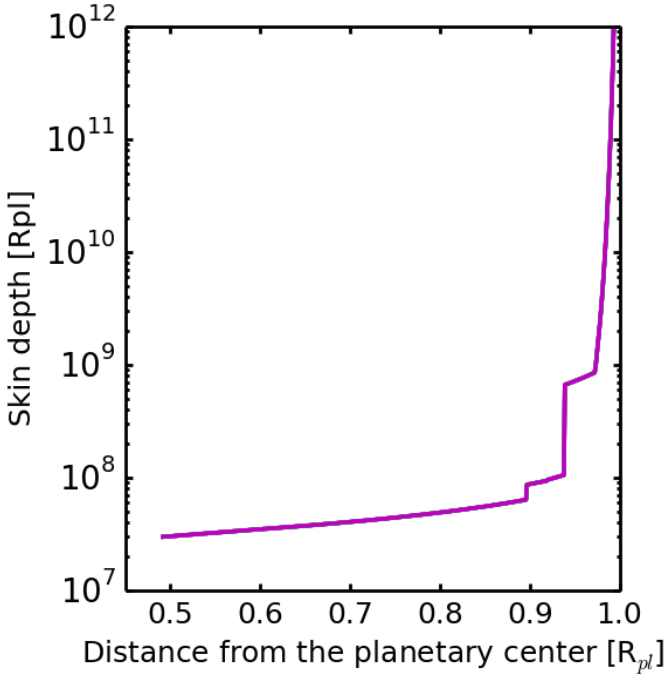

Figure 14: Skin depth of an Earth-like planet. As explained in chapter 2, the skin depth determines the penetration depth of the variable external electromagnetic field inside the body (Rudnev 2003). The skin depth is the same for all eccentricities because the orbital period and therefor the magnetic field variation frequency also is the same.

4. Discussion

The investigation of the planets orbiting TRAPPIST-1 and WX UMa is based on the assumption that they have no internal dynamo and thus no magnetic field. Furthermore, no global resurfacing or plate tectonics is assumed as a heat-removing mechanism (Breuer & Moore 2015). At present, its is not possible to determine the tectonic mode of an exoplanet. For terrestrial planets and moons, based on the strong dependence of the planet's mantle viscosity on the temperature, it is conservatively assumed that stagnant lid is the most common tectonic mode. Due to a lack of detailed information on geological activities of exoplanets and the seemingly limiting occurrence of plate tectonics in the solar system bodies, stagnant lid may be considered the most common tectonic mode of terrestrial planets (Christensen 1984, Davaille & Jaupart 1993, Solomatov 1995). In our solar system, all terrestrial planet excluding Earth are currently in the stagnant lid regime. It is suggested that one-time or repeated global resurfacing events have occurred on Venus in the past (Strom et al.1994). Mercury, Mars, and the Moon have probably spent the majority of their lifetimes in the stagnant lid regime (Noack et al. 2012, Turcotte 1993).

A stagnant lid, which could occur on a variety of exoplanets and exomoons, is a solid layer of silicate minerals over a convective interior. Thus, the mantle lacks a strong cooling mechanism, as in active plate tectonics. The onset of plate tectonics is highly dependent on the temperature and viscosity of the planetary mantle, the water content and the mantle rheology (Stamenković & Breuer 2014, Noack and Breuer 2014). Plate tectonics becomes more probable with decreasing temperature and increasing viscosity of a highly convective mantle. It is possible that the temperature increase of planetary interiors due to induction heating can prevent the onset of plate tectonics. However, additional studies are necessary to determine the role of induction heating and other heating mechanisms for plate tectonics. The mantle melting can be prevented when active plate tectonics is present, but that the surface stays solid even if there is a subsurface magma ocean (Stamenković & Breuer 2014).

The thorough investigation of operating tectonic mode, volcanic activity and resurfacing on the habitability of a planet is of fundamental importance for exploration of exoplanetary systems, as well as our own. On the planet Earth, the carbon-silicate cycle is operating due to plate tectonics, whereby geochemical transformation processes regulate the atmospheric content of carbon over geological timescales and thus contribute to the stability of the global climate (Tosi et al. 2017, Walker et al. 1981, Kasting et al. 1993). It depends on many factors, whether and how long life can arise and exist on a planet or moon. Even Earth could develop into a cold, uninhabitable body by reducing the rate of carbon dioxide degassing from the planet's interior, despite prevailing plate tectonics (Tajika 2007, Kadoya & Tajika 2014, 2015). Volcanic degassing of effective greenhouse gases H_2O and CO_2 determine the composition as well as the evolution of the atmosphere and the surface temperature (Kasting et al. 1993; Kopparapu et al. 2013). If the degassing rate of an Earth-like planet falls below a critical value, the existing climate mode can change from a warm state to a snowball state. A temperate surface, which allows the presence of water in liquid form, would transform into a global ice desert that harbors inner oceans under its ice crust (Tajika 2008). The content of carbon in the mantle of a planet and the generation depth of the melt determine the degassing rate of carbon dioxide (Tajika & Matsui 1992). Too much outgassing and extreme volcanic activity can be equally bad for habitability (Tajika 2008). Volcanism and the resulting degassing occurs, both on planets with plate tectonics, and those whose tectonic mode is the stagnant lid, and de-

pends heavily on the internal activity, especially on the thermal evolution of the mantle (Kadoya & Tajika 2014, Tosi et al. 2017). The exact location of a planet within the circumstellar habitable zone plays a fundamental role in its planetary habitability (Kasting et al. 1993, Selsis et al. 2007). The inner boundary of the habitable zone, closer to the star, is defined as the orbital distance, where the runaway greenhouse effect evaporates all surface water (Lammer et al. 2009). In addition, the photodissociation of water vapor into molecular hydrogen (H2) and molecular oxygen (O2) in the upper atmosphere of a planet, which allows the hydrogen to escape (Lammer et al. 2009). If a planet is very close to the star, closer than the inner boundary of the habitable zone, Venus-like atmospheric states could dominate. No liquid water would be found on this surface (Solomon & Head 1991).

Observations of the Jovian satellite Io showed that tidal forces caused by the close orbit around Jupiter and the gravitational effects of the moons Europa and Ganymede influence this Jupiter's moon. Io has no liquid water on its surface and certainly not able to sustain life. Io's strong volcanic activities lead to a sulfur dioxide outgassing. This volcanism is explained by the close eccentric orbit of Io and the resulting varying gravitational force of Jupiter. The interior of the moon is exposed to friction, which results in tidal heating. The orbits of Ganymede, Europe and Io show a 4:2:1 resonance, which forces Io's orbit to be elliptical. Since this Laplace resonance leads to a cyclic line up of the three Jupiter moons (Catling 2013). In addition, due to the eccentric orbit, Io experiences a varying magnetic field from Jupiter in its orbital motion. Therefore, part of the internal energy is to be attributed to induction heating. So, induction heating of Io’s mantle contributes to the fact that this moon has the strongest volcanic activity in the solar system (Goldreich & Lynden-Bell 1969, Colburn 1980, Spencer et al. 2000, Davies 2007). Io's volcanism allows high outgassing of sulfur and oxygen. Due to the atmospheric escape, a torus of plasma has formed along the orbit (Steffl et al. 2013). Our result show that induction heating and the resulting energy releases in the planetary mantle can lead to volcanic activity far surpassing Io’s.

The surface conditions of a planet can be influenced by endogenous and exogenous processes. Volcanism and tectonics are caused by internal processes of the planet. Effects of the magnetic field, solar wind or cratering are among the exogenous influences (Hartmann 1983, p. 343). Volcanic activities, which are induced by induction heating, represent a combination of these internal and external processes of surface evolution. Many internal processes have been extensively studied before, but the induction heating is a newly considered mechanism for exoplanets, which makes our studies important.

In this thesis, I have shown that induction heating is not substantial in the TRAPPIST-1 system, if the variation of the magnetic field is generated due to orbital eccentricities alone. TRAPPIST-1 has a magnetic field of 600 G (Reiners & Basri 2010). I have shown that the internal energy release generated by induction heating reaches values between $7.5 * 10^{17}$ ergs / s for TRAPPIST-1b and $1.1 * 10^{12}$ergs / s for TRAPPIST-1h, this is due to a relatively small magnetic field of the star and small orbital eccentricities. According to Luger et al (2017), the main source of internal energy of these exoplanets is tidal heating. The tidal heat flux of TRAPPIST-1b, TRAPPIST-1c, TRAPPIST-1d, TRAPPIST-1e and TRAPPIST-1g each exceeds the total heat flux of the Earth. According to Barr et al's (2018) model, the tidal heat flux values of the innermost four planets in the TRAPPIST-1 system are more than twenty times the mean heat flux of the Earth.

On the other hand, the energy release in a test planet orbiting WX UMa was very high for high eccentricities. The internal energy levels produced by induction heating in the planet orbiting WX UMa are significant for higher eccentricities. The orbit had eccentricities between 0.1 and 0.9 and a distance of 0.05 AU to WX UMa in its HZ. The dipole and rotational axes of WX UMa and TRAPPIST-1 were aligned for the calculations in my model so that the planets experience a varying strong magnetic flux related to the orbital eccentricity and the strength of the stellar magnetic field. The internal energy generated by induction heating and the associated volcanism and the outgassing of planets with eccentricities of 0.4 and 0.5 equal the internal energy release of the Earth by radioactive decay of $2.1 * 10^{20}$ ergs / s. The release of the internal energy of the test planet with eccentricities above 0.6 exceeds the volcanic activity of Io (Schubert et al. 2004). The 7300 G magnetic field of the M dwarf WX UMa is one of the strongest which has been measured so far around stars of this class (Shulyak et al. 2017).

My calculation show that the magnitude of the induction heating depends both on the stellar magnetic field strength and on the eccentricity of the planetary orbit. Induction heating in planets with an eccentric orbit that experience a varying stellar magnetic field can cause sub-surface magma oceans to trigger massive volcanic activity. On the one hand, released greenhouse gases can have a positive effect by maintaining or filling the atmosphere, and on the other, greenhouse gases affect the planet's climate. Resulting temperature differences can adversely affect the habitability of a planet (McEwen et al. 1998, Alberti et al. 2017, Wolf 2017).

With the help of Dr Kristina Kislyakova it was possible for me to develop a new model which takes into account different frequencies present in the orbital motion. This model is applicable to complicated systems with multiple planets including gas giants, where the orbits of smaller planets are disturbed by the gravitational influences of the giants. This leads to the orbital motion where the orbital phase can not be described by a simple sinus anymore, but takes a more complicated form. This model takes this into account and allows to calculate induction heating in such systems.

5. Conclusion

Recent discoveries of exceptionally strong magnetic fields around M stars (Shulyak et al. 2017) inspired the studies on the induction heating of orbiting planets in the habitable zone. The contribution of induction heating to the evolution of a planet and its habitability should be included in studies on evolution of exoplanets (Kislyakova et al. 2017 & 2018). Induction heating can occur inside planets that move in eccentric orbits. Due to the changing distance to the central star, a periodically varying magnetic field acts on the exoplanet. When the planet is embedded into a varying field, it is subject to electromagnetic induction heating of interiors. The magnitude of the effect can vary from barely perceptible warming in the mantle to extreme volcanic activity and periodic global resurfacing.

Of particular interest here are long-lived M dwarf stars with strong magnetic fields. These small and cool stars represent the largest population of stars in our galaxy. This group of stars also has very active members with magnetic fields up to several kilogauss. Most of the fully convective M stars are fast rotators and produce strong magnetic fields with dipole-dominated geometries (Shulyak et al. 2017). The focus of the investigation here are M dwarfs whose planets are small, rocky planets that could only be detected in recent times. In this work, induction heating in the seven TRAPPIST-1 planets and inside a test planet orbiting WX UMa is calculated, assuming different planetary eccentricities. To study internal energy release by induction heating in planets on eccentric orbits experiencing a varying magnetic field, this two systems were compared. The planets in the TRAPPIST-1 system have low eccentricities and are exposed to a 600 G stellar magnetic field (Reiners & Basri 2010). In contrast, WX UMa has a magnetic field of 7.3 kG (Shulyak et al.2017) and is orbited by a test planet with eccentricities between 0.1 and 0.9.

To investigate the effects of the exceptionally strong WX UMa magnetosphere on a terrestrial planet with eccentric orbit, I have modified and applied the model by Kislyakova et al. 2017 & 2018. The magnetic field of the fast-rotating M dwarf WX UMa shows a distinct dipole component. Due to the co-alignment of the axis of rotation and the dipole axis of this low-mass main-sequence stars, the orbit must be either inclined or eccentric for the planet to be exposed to a varying magnetic flux in its orbital motion (Laine & Lin 2012, Buzasi 2013, Shulyak et al. 2017). If we assume that the dipole and rotational axes of TRAPPIST-1 are similarly inclined as is the case for WX UMa, the orbiting planets experienced a magnetic field variation due to the eccentric planetary orbits in my model.

According to Kislyakova et al. 2017 induction heating had a significant impact on the condition of their interior energy and resulting surface conditions of the four innermost exoplanets, TRAPPIST-1b, -1c, -1d and -1e, if an angle of 60 degrees is assumed between the magnetic field axis and the dipole axis. I have shown that the heat flux produced by induction heating of the planetary mantle of the exoplanets in the TRAPPIST-1 system is not significant, if the energy release is due to the eccentricities of the planents' orbits. Therefore, a conclusion follows that an inclined stellar dipole is necessary for the induction heating to be substantial, and the observed planetary eccentricities are not big enough for a substantial effect. The internal energy release by induction heating of the planets 1b-1h reaches values between $7.5 * 10^{17}$ ergs / s for TRAPPIST-1b and $1.1 * 10^{12}$ergs / s for TRAPPIST-1h. Thus, the results are well below the internal energy release of the Earth by radioactive decay of $2.1 * 10^{20}$ ergs / s (Schubert et al 2001). The majority of internal energy in TRAPPIST-1's planets is generated

by tidal heating, which is due to a relatively small magnetic field of the star and small orbital eccentricities (Luger et al., 2017). In contrast, the values of internal energy generated by induction heating for the test planet orbiting WX UMa are significant for higher eccentricities. In my model, orbital motions with eccentricities between 0.1 and 0.9 were simulated. The orbit of the Earth-like planet lay in the circumstellar habitable zone. WX UMa's magnetic field is approximately 7300 G (Shulyak et al.2017). The rotation and dipole axes of WX Uma and TRAPPIST-1 are co-aligned for the calculations in my model, so the planets experience a varying stellar magnetic flux, which is related only to the eccentricity of the planetary orbit and the strength of the stellar magnetic field. The internal energy generated by induction heating in the planetary interior on its eccentric orbital motion and the associated volcanism and the outgassing of planets with an eccentricities of 0.4 and 0.5 equal the internal energy release of the Earth by radioactive decay. The internal energy release of the test planet with eccentricities beyond 0.6 surpass the Jupiter's moon, Io of activity (Schubert et al. 2004). Induction heating can drive strong volcanic activity (Kislyakova et al. 2017 & 2018).

If the atmosphere of a planet is subject to strong atmospheric losses, a plasma torus of a volcanic origin can form along the orbit. Depending on volcanic degassing composition, the torus that the active planet generates, consists of such elements as sulfur and oxygen, as is the case with Io. Planets or moons, where carbon dioxide is outgassed by volcanic eruptions, could form a plasma torus of carbon (Haswell et al. 2012, Fossati et al., 2013). Kislyakova et al (2018) have shown that such a torus would be observable in the ultraviolet wavelengths around nearby stars.

In conclusion, our study shows that induction heating can be very strong in planets on eccentric orbits around stars with strong magnetic fields even for planets in the habitable zones. These results are of big importance for the future habitability studies of planets orbiting active M-stars. Since the increased outgassing of carbon dioxide and other greenhouse gases from the interiors has a major influence on the planetary climate, it is obvious that induction heating of the mantle is a significant factor for the habitability of a planet (Alberti et al. 2017, Wolf 2017).

6. Abstract

If a planet is embedded in a varying field, it is subject to electromagnetic induction heating of interiors. Internal energy release through induction heating can range from barely perceptible warming in the mantle to extreme volcanic activity and outgassing. Increased outgassing of greenhouse gases, like CO_2 from the inside has a fundamental impact on the Earth's climate, so it is obvious that the induction heating of the mantle is an important factor in the habitability of an exoplanet (Alberti et al. 2017, Wolf 2017).

In order to demonstrate the crucial influence of eccentricity on induction heating of the planetary mantle, we have tested different eccentricities ranging from $0.1 < e < 0.9$ for a test planet orbiting WX UMa. The magnetic field of WX UMa is 7.3 kG (Shulyak et al. 2017). On the other hand we have simulated the effect of induction heating of the planets of TRAPPIST-1. TRAPPIST-1 has a magnetic field of 600 G (Reiners & Basri 2010) and seven rocky planets orbiting the star with low eccentricities. My calculations show that while the effect is not significant in the TRAPPIST-1 system, it is of extreme importance for a test planet around WX UMa, if it has high eccentricities.

According to my model, the internal energy release by induction heating of TRAPPIST-1b, the innermost planet in this system, corresponds to $7.5 * 10^{17}$ ergs / s. The value for the internal energy release of the Earth by radioactive decay is $2.1 * 10^{20}$ ergs / s. This value is exceeded for the test planet orbiting WX UMa with an eccentricity $e > 0.5$. The high frequency of magnetic flux variations experienced by the test planet orbiting WX UMA at higher eccentricities would create volcanism that would exceed the Jupiter's moon, Io in terms of activity. Induction heating is an important source of internal energy for close-in exoplanets on eccentric orbits in the habitable zone of M dwarfs with a strong magnetic field. The energy release due to induction heating can lead to sub-surface magma oceans triggering massive volcanic activity. Greenhouse gases, which are released, can have a positive effect by preserving or filling the atmosphere. The proportion of greenhouse gases has a direct impact on the planetary climate. The global climate can create non-habitable conditions on a planets surface (McEwen et al 1998, Alberti et al 2017, Wolf 2017).

7. Zusammenfassung (Deutsch)

Wenn ein Planet in ein variierendes Magnetfeld eingebettet ist, unterliegt er einer elektromagnetischen Induktionserwärmung. Die innere Energiefreisetzung durch Induktionserwärmung kann von kaum wahrnehmbarer Erwärmung im Mantel bis hin zu extremer Vulkanaktivität und Ausgasung reichen. Eine erhöhte Ausgasung von Treibhausgasen wie Kohlendioxid hat einen grundlegenden Einfluss auf das Erdklima. Es ist daher offensichtlich, dass die Induktionsheizung des Mantels ein wichtiger Faktor für die Bewohnbarkeit eines Exoplaneten sein kann (Alberti et al. 2017, Wolf 2017).

Um den entscheidenden Einfluss der Exzentrizität auf die Induktionsheizung des Planetenmantels zu demonstrieren, haben wir verschiedene Exzentrizitäten im Bereich von $0,1 < e < 0,9$ für einen Testplaneten getestet, der WX UMa umkreist. Das Magnetfeld von WX UMa beträgt 7,3 kG (Shulyak et al. 2017). Auf der anderen Seite haben wir den Effekt der Induktionsheizung der Planeten von TRAPPIST-1 simuliert. TRAPPIST-1 hat ein Magnetfeld von 600 G (Reiners & Basri 2010) und sieben felsige Planeten, die den Stern mit geringen Exzentrizitäten umkreisen. Meine Berechnungen zeigen, dass der Effekt im TRAPPIST-1-System zwar nicht signifikant ist, aber für einen Testplaneten um WX UMa von äußerster Wichtigkeit ist, wenn er hohe Exzentrizitäten aufweist.

Gemäß meinem Modell entspricht die innere Energiefreisetzung durch Induktionserwärmung von TRAPPIST-1b, dem innersten Planeten in diesem System, $7.5 * 10^{17}$ erg / s. Der Wert für die innere Energiefreisetzung der Erde durch radioaktiven Zerfall ist $2.1 * 10^{20}$ ergs / s. Dieser Wert wird für den Testplaneten WX UMa mit einer Exzentrizität $e > 0,5$ überschritten. Die hohe Frequenz von Magnetfluss Schwankungen, die der Testplanet erfährt, wenn er WX UMA bei höheren Exzentrizitäten umkreist, würde einen Vulkanismus erzeugen, der den Jupitermond Io in Bezug auf die Aktivität übersteigen würde. Induktionsheizung ist eine wichtige Quelle für innere Energie für nahegelegene Exoplaneten auf exzentrischen Bahnen in der bewohnbaren Zone von M Zwergen mit einem starken Magnetfeld. Die Energiefreisetzung aufgrund von Induktionserwärmung kann dazu führen, dass Magma-Ozeane unter der Oberfläche massive Vulkanaktivitäten auslösen. Treibhausgase, die freigesetzt werden, können sich positiv auf die Erhaltung oder Anreicherung der Atmosphäre auswirken. Der Anteil der Treibhausgase hat einen direkten Einfluss auf das Klima eines Planeten. Das globale Klima kann nicht bewohnbare Bedingungen auf einer Planetenoberfläche schaffen (McEwen et al. 1998, Alberti et al. 2017, Wolf 2017).

Acknowledgments

I would like to thank Dr Kristina G. Kislyakova from the University of Vienna, Department of Astrophysics, Türkenschanzstrasse 17, A-1180, Vienna, Austria for the opportunity to shed light on this topic and for the cordial and professional support in programming and coding! The basic program that I have changed is due to my supervisor Dr Kristina G. Kislyakova. I owe Mag Dr Elke Pilat-Lohinger from the University of Vienna, Department of Astrophysics, Türkenschanzstrasse 17, A-1180, Vienna, Austria, the orbital calculations for the test planet of WX UMa. I would also like to thank DI Nick Mayerhofer for his expert support in programming and coding.

Special thanks to my husband.

References

Alberti, T., Carbone, V., Lepreti, F. & Vecchio, A. (2017): Comparative climates of TRAPPIST-1 planetary system: results from a simple climate–vegetation model. ApJ. 844, 19.

Altschuler, M. D., & Newkirk, G. (1969): Magnetic fields and the structure of the solar corona. I: Methods of calculating corona fields, Sol. Phys., 9, 131-149.

Anderson JD1, Schubert G, Jacobson RA, Lau EL, Moore WB, Sjogren WL (1998): Europa's differentiated internal structure: inferences from four Galileo encounters, Science, 4.1c.

Barnes, S. A. (2003): A Connection between the Morphology of the X-Ray Emission and Rotation for Solar-Type Stars in Open Clusters, ApJ, 586, 464.

Barr, A. C., et al. (2018): Interior structures and tidal heating in the TRAPPIST-1 planets A&A, Vol 613, Nr. A37, 13.

Barry, D. C. (1988): The chromospheric age dependence of the birthrate, composition, motions, and rotation of late F and G dwarfs within 25 parsecs of the sun, ApJ, 334, 436.

Beech, M. (2011): Since When Was the Sun a Typical Star? J. R. Astron. Soc. Can., 105, 232.

Belley, F. et al. (2009): The magnetic properties of natural and synthetic $(Fe_x, Mg_{1-x})_2SiO_4$ olivines. Earth Planet. Sci. Lett. 284, 516–526.

Berge, G. L. (1965): An interferometric study of Jupiter at 10 and 21cm. Radio Sci. 69D: 1552-1556.

Berge, G. L. (1966): An interferometric study of Jupiter’s decimetric radio emission, ApJ, 146, 767-798.

Berger, E., et al. (2008): Simultaneous multiwavelength observations of magnetic activity in ultracool dwarfs. I. The complex behavior of the M8. 5 dwarf TVLM 513–46546, ApJ, 673, 1080.

Berta, Z. K., Irwin, J., Charbonneau, D., Burke, C. J., & Falco, E. E. (2012): Transit detection in the MEarth survey of nearby M dwarfs: bridging the clean-first, search-later divide, AJ, 144, 145.

Breuer, D. & Moore, B. (2015): Dynamics and thermal history of the terrestrial planets, the Moon, and Io. Physics of Terrestrial Planets and Moons 10, p. 255–305.

Bolmont E., Selsis F., Owen J. E. et al (2017): Water loss from terrestrial planets orbiting ultracool dwarfs: implications for the planets of TRAPPIST-1, MNRAS 464 3728

Bonura, T., Smith, K.C., (1975a): Enzymatic production of deoxyribonucleic acid double-strand
breaks after ultraviolet irradiation of Escherichia coliK-12. J. Bacteriol. 121, 511–517.

Bonura, T., Smith, K.C., (1975b): Quantitative evidence for enzymatically-induced DNA double- strand breaks as lethal lesions in UV-irradiated pol+ and polA1 strains of E. coli K-12. Photochem. Photobiol. 22, 243–248.

Borucki, W.J., et al., (2011): Characteristics of planetary candidates observed by Kepler. II. analysis of the first four months of data. ApJ. 736 (July), 19.

Broda W. (2007): Astronomischer Berechnungscocktail, Ein ABC der Himmelsmechanik; Oculum Verlag, 1. Auflage, Seite 209, 223-225.

Burgasser A. J. and Mamajek E. E. (2017): The age of the TRAPPIST-1 system; ApJ, Vol 845, Nr.2.

Buzasi, D. (2013): Stellar magnetic fields as a heating source for extrasolar giant planets, ApJL, 765, L25.

Carr T. D. and Gulkis S. (1969): The magnetosphere of Jupiter, Ann. Rev. A&A 7. 577.

Carr, M. H. et al. (1998): Evidence for a subsurface ocean on Europa. Nature 391, 363–365.

Catling, D. C., (2013): Astrobiology: A Very Short Introduction Oxford OUP.

Chabier & Baraffe (1997): Structure and evolution of low-mass stars, A&A, v.327, p. 1039-1053.

Charbonneau, P., Christensen-Dalsgaard, J., Henning, R., et al. (1999): Helioseismic constraints on the structure of the solar tachocline, ApJ, 527, 445.

Charbonneau, D., Berta, Z.K., Irwin, J., Burke, C.J., Nutzman, P., Buchhave, L.A., Lovis,

C., Bonfils, X., Latham, D.W., Udry, S., Murray-Clay, R.A., Holman, M.J., Falco, E.E., Winn, J.N., Queloz, D., Pepe, F., Mayor, M., Delfosse, X., Forveille, T. (2009): A super-Earth transiting a nearby low-mass star. Nature 462 (December), 891–894.

Christensen, U. R. (1984): Convection with pressure-and temperature-dependent non-Newtonian rheology, Geophys. J. R. Astr. Soc., 77, 343.

Colburn, D. S. (1980): Electromagnetic heating of Io, J. Geophys. Res. 85, 7257–7261.

Cooley, J. W., & Tukey, J. W. (1965): An algorithm for the machine calculation of complex Fourier series. Mathematics of computation, 19(90), 297-301.

Corbard, T., Berthomieu, G., Provost, J., & Morel, P. (1998): Inferring the equatorial solar tachocline from frequency splittings, A&A, 330, 1149-1159.

Corbard, T., Jim´enez-Reyes, S. J., Tomczyk, S., Dikpati, M., & Gilman, P. (2001): in Helio- and Asteroseismology at the Dawn of the Millennium (ESA Publ. SP-464), 265–272.

Dartnell, L.R., (2011): Ionizing radiation and life. Astrobiology 11, 551–582.

Davaille, A., & Jaupart, C. (1993): Transient high Rayleigh number convection with large viscosity variations., J. Fluid Mech., 253, 141.

DellaGiustina D. (2017): Developing a Method to Determine Electrical Conductivity in Meteoritic Materials with Applications to Induction Heating Theory (2008 Student Thesis), eprint arXiv:1707.07648.

Delrez, L., Gillon, M., H.M.J, Amaury; et al. (April 2018). "Early 2017 observations of TRAPPIST-1 with Spitzer". Monthly Notices of the Royal Astronomical Society. 475 (3): 3577–3597.

Demtröder Experimentalphysik 2 (2006): Elektrizität und Optik,Springer Verlag, 4. Auflage, p. 123-135.

Dole, S.H. (1964): Habitable Planets for Man, Blaisdell Publishing, New York.

Doyle, L.R., McKay, C.P., Whitmire, D.P., Matese, J.J., Reynolds, R.T., and Davis, W.L. (1993): Astrophysical constraints on exobiological habitats. In ASP Conference Series, Vol. 47: Third Decennial US-USSR Conference on SETI, edited by G.S. Shostak, Astronomical Society of the Pacific, San Francisco, pp. 199–217.

Dressing, C. D., & Charbonneau, D. (2013): The Occurrence Rate of Small Planets around Small Stars, ApJ, 767, 95.

Dressing, C. D., & Charbonneau, D. (2015): The Occurrence of Potentially Habitable Planets Orbiting M Dwarfs Estimated from the Full Kepler Dataset and Empirical Measurement of the Detection Sensitivity, ApJ, 807, 45.

Endl, M., Cochran, W.D., Tull, R.G., and MacQueen, P.J. (2003): A dedicated M dwarf planet search using the Hobby-Eberly Telescope. A J. 126, 3099–3107.

Ferré, E. C. et al. (2014); Eight good reasons why the uppermost mantle could be magnetic. Tectonophysics 624, 3–14.

Field G. and Chaisson E. (2013): Das unsichtbare Universum: An den Grenzen der modernen Astrophysik, Springer Verlag, p. 85.

Fossati, L., Ayres, T. R., Haswell, C. A., et al. (2013): Absorbing Gas around the WASP-12 Planetary System, ApJL, 766, L20.

Ferraz-Mello, S., Rodr´ıguez, A. & Hussmann, H. (2008): Tidal friction in close-in satellites and exoplanets: The Darwin theory re-visited. Celest. Mech. Dyn. Astr. 101, 171–201.

Gaillard, F. & Iacono Marziano, G. (2005): Electrical conductivity of magma in the course of crystallization controlled by their residual liquid composition. J. Geophys. Res. 110, B06204.

Garraffo C. (2015): Magnetic complexity as an explanation for bimodal rotation population among young stars, ApJL, Vol 807, Issue 1, L6.

Garraffo C., Drake J. J. and Cohen O. (2016): The Space Weather of Proxima Centauri b, ApJL 833 L4

Garraffo Cecilia, Jeremy J. Drake1, Ofer Cohen1,2, Julian D. Alvarado-Gómez1, and Sofia P. Moschou (2017): The Threatening Magnetic and Plasma Environment of the TRAPPIST-1 Planets, ApJL, Vol. 843, Nr. 2.

Gershberg, R.E., Katsova, M.M., Lovkaya, M., Terebizh, A.V., and Shakhovskaya, N.I. (1999): Catalogue and bibliography of the UV Ceti-type flare stars and related objects in the solar vicinity. Astron. Astrophys. Suppl. Ser. 139, 555–558.

Gillon, M., Jehin, E., Lederer, S. M., et al. (2016): Temperate Earth-sized planets transiting a nearby ultracool dwarf star, Nature, 533, 221.

Gillon, M., Triaud, A. H. M. J., Demory, B.-O., et al. (2017): Seven temperate terrestrial planets around the nearby ultracool dwarf star TRAPPIST-1, Nature, 542, 456.

Gizis, J. E., Monet, D. G., Reid, I. N., et al. (2000): New Neighbors From 2MASS: Activity and Kinematics at the Bottom of the Main Sequence, AJ, 120, 1085.

Goldreich, P. & Lynden-Bell, D. (1969): Io, a jovian unipolar inductor. ApJ 156, 59–78.

Gregory, S. G. & Donati, J.-F. (2011): Analytic and numerical models of the 3D multipolar magnetospheres of pre-main sequence stars. Astron. Nachr. 332, p. 1027.

Grenfell, J. L., Rauer, H., Selsis, F., et al. (2010): Co-evolution of atmospheres, life, and climate, Astrobiology, 10, 77.

Grießmeier, J.-M., Stadelmann, A., Grenfell, J. L., Lammer, H., & Motschmann, U. (2009): On the protection of extrasolar Earth-like planets around K/M stars against galactic cosmic rays, Icarus, 199, 526.

Grießmeier, J.-M., Stadelmann, A., Motschmann, U., et al. (2005): Cosmic ray impact on extrasolar Earth-like planets in close-in habitable zones, Astrobiology, 5, 587.

Grimm S. L. et al. (2018): The nature of TRAPPIST-1 exoplanets, Astronomy & Astrophysics manuscript no. trappist1 February 6, A&A 613, A68.

Gough, D. O. (1981): Solar interior structure and luminosity variations, Sol. Phys., 74, 21.

Guedel M, Dvorak R, Erkaev N, Kasting J, Khodachenko M, et al. (2014): Astrophysical conditions for planetary habitability, Protostars and Planets VI, Henrik Beuther, Ralf S. Klessen, Cornelis P. Dullemond, and Thomas Henning (eds.), University of Arizona Press, Tucson, 914 pp., p.883-906.

Günther, A. (2003): Magnetische Anisotropie gebänderter Eisenerze und deren Beziehung zu kristallographischen Vorzugsrichtungen. Diss. Univ. Clausthal; S157, Clausthal.

Gurzadyan G. A. (1980): Flare Stars: International Series in Natural Philosophy.

Haberle, R.M., McKay, C., Tyler, D., and Reynolds, R. (1996): Can synchronous rotating planets support an atmosphere? In Circumstellar Habitable Zones, edited by L.R. Doyle, Travis House, Menlo Park, CA, pp. 29–41.

Harris, D. L. (1961): Photometry and colorimetry of planets and satellites. In Planets and Satellites (Kuiper, G. P., and Middlehurst, B. M., eds.) Univ. of Chicago Press, pp. 272- 342.

Hart, M.H. (1979): Habitable zones about main sequence stars. Icarus 37, 351–357.

Hartmann K. William (1983): Moons and Planets, Wadsworth Publishing Company, Second Edition, page 255, 262-263, 265.

Haswell, C. A., Fossati, L., Ayres, T., et al. (2012): Near-Ultraviolet Absorption, chromospheric activity, and Star-Planet Interaction in the WASP-12 System, ApJ, 760, 79.

Hawley, S. L., Gizis, J. E., & Reid, I. N. (1996): The Palomar/MSU nearby star spectroscopic survey. II. The southern M dwarfs and investigation of magnetic activity, AJ, 112, 2799.

Hawley Suzanne L, Davenport James R. A. (2014): Kepler Flares I. Active and inactive M dwarfs, https://arxiv.org/abs/1410.7779.

Hilton, E. J. (2011): The Galactic M Dwarf Flare Rate - SAO/NASA ADS, PhD thesis, University of Washington

Horneck, G., Walter, N., Westall, F., et al. (2016): AstRoMap European astrobiology roadmap, Astrobiology, 16, 201

Irwin, J., et al. (2009b): GJ 3236: A new bright, very low mass eclipsing binary system discovered by the MEarth Observatory, ApJ, 701, 1436.

Irwin, J. M., et al. (2011b): LSPM J1112+ 7626: Detection of a 41 Day M-dwarf Eclipsing Binary from the MEarth Transit Survey, ApJ, 742, 123.

ISO 21348 1. Mai (2007): Space environment (natural and artificial) — Process for determining solar irradiances.

Jacobsen, S. B. (2005): The Hf-W / Isotopic System and the Origin of the Earth and Moon, Annual Review of Earth and Planetary Sciences, Vol. 33:531-570.

Jardine, M., Barnes, J. R., Donati, J., & Collier Cameron, A. (1999): Coronal emission and dynamo saturation, MNRAS, 305, L35.

Joshi, M. (2003): Climate model studies of synchronously rotating planets. Astrobiology 3, 415–427.

Joshi, M.M., Haberle, R.M., and Reynolds, R.T. (1997): Simulations of the atmospheres of synchronously rotating terrestrial planets orbiting M dwarfs: conditions for atmospheric collapse and the implications for habitability. Icarus 129, 450–465.

Joy, A.H., (1967): , ASPL, 10, 41 (BIBCODE:1967ASPL…10...41J).

Kadoya, S., & Tajika, E. (2014): Conditions for Oceans on Earth-Like Planets Orbiting within the Habitable Zone: Importance of Volcanic CO2 degassing, ApJ, 790, 107.

Kadoya, S., & Tajika, E. (2015): Evolutionary Climate Tracks of Earth-Like Planets, ApJ, 815, L7.

Kasting, J.F., Whitmire, D.P., Reynolds, R.T., (1993): Habitable zones around main sequence stars. Icarus 101 (January), 108–128.

Khodachenko, M. L., Ribas, I., Lammer, H., et al. (2007): Coronal mass ejection (CME) activity of low mass M stars as an important factor for the habitability of terrestrial exoplanets. I. CME impact on expected magnetospheres of Earth-like exoplanets in close-in habitable zones, Astrobiology, 7, 167.

Khurana, K. K., Walker, R. J., Ogino, T. (1996): Magnetospheric convection in the presence of interplanetary magnetic field By: A conceptual model and simulations, Jour. Geophys. Res.: Space Physics, Vol. 101, Issue A3.

Khurana K. K. et al. (2009): Electromagnetic Induction from Europa's Oceans and the Deep Interior 585.

Kislyakova K. G., L. Noack, C. P. Johnstone, V. V. Zaitsev, L. Fossati, H. Lammer, M. L. Khodachenko, P. Odert, M. Guedel (2017): Magma oceans and enhanced volcanism on TRAPPIST-1 planets due to induction heating, https://arxiv.org/abs/1710.08761.

Kislyakova K. G., L. Fossati2 , C. P. Johnstone1 , L. Noack3 , T. Lüftinger1, V. V. Zaitsev4, and H. Lamm (2018): Effective Induction Heating around Strongly Magnetized Stars, https://arxiv.org/abs/1804.06346.

Kivelson, M. G. et al. (1997): Europa's magnetic signature: report from Galileo's first pass on December 19, 1996. Science 276, 1239–1241.

Kivelson, M. G. (1996): Discovery of Ganymede's magnetic field by the Galileo spacecraft. Nature 384, 537– 54.

Kivelson, M. G. et al. (1996): A magnetic signature at Io: initial report from the Gallileo magnetometer. Science 273, 337–340.

Kopparapu, R. K., Ramirez, R., Kasting, J. F., et al. (2013): Habitable zones around main-sequence stars: new estimates, ApJ, 765, 131.

Johnstone, C. P. (2012): Magnetic Fields and X-ray Emission in Pre-Main Sequence Stars. PhD thesis, Univ. St Andrews.

Laine, R. O., & Lin, D. N. C. (2012): Interaction of close-in planets with the magnetosphere of their host stars. II. Super-Earths as unipolar inductors and their orbital evolution, ApJ, 745, 2.

Lammer, H., Lichtenegger, H. I. M., Kulikov, Y. N., et al. (2007): Coronal Mass Ejection (CME) Activity of Low Mass M Stars as An Important Factor for The Habitability of Terrestrial Exoplanets. II. CME-Induced Ion Pick Up of Earth-like Exoplanets in Close-In Habitable Zones Astrobiology, 7, p. 185.

Lammer, H., J. F. Kasting, E. Chassefie`re, R. E. Johnson, Yu. N. Kulikov, and F. (2008): Tian, Atmospheric escape and evolution of terrestrial planets and satellites, Space Sci. Rev., 139, 399–436.

Lammer, H., J. H. Bredeho¨ft, A. Coustenis, M. L. Khodachenko, L. Kaltenegger, O. Grasset, D. Prieur, F. Raulin, P. Ehrenfreund, M. Ya- mauchi, J.-E. Wahlund, J.-M. Grießmeier, G. Stangl, C. S. Cockell, Yu. N. Kulikov, L. Grenfell, and H. Rauer (2009): What makes a planet habitable?, A&A,17,181–249.

Larmor, J. (1919): How Could a Rotating Body Such as the Sun Become a Magnet? Reports of the British Association, 87, 159-160.

Luger R. et al. (2017): A seven-planet resonant chain in TRAPPIST-1, Nature Astronomy 1, 0129.

Lundin, R., Lammer, H., & Ribas, I. (2007): Planetary Magnetic Fields and Solar Forcing: Implications for Atmospheric Evolution, Space Sci. Rev., 129, 245.

Mackay, D. H., Priest, E. R. & Lockwood, M. (2002): The evolution of the Sun's open magnetic flux—II. Full solar cycle simulations. Solar. Phys. 209, 287–309.

Marcy, G.W., Butler, R.P., Vogt, S., and Shirts, P. (1998): The Keck search for extrasolar planets. Bull. Am. Astron. Soc. 30, 825.

Markey, P., & Tayler, R. J. (1973): The adiabatic stability of stars containing magnetic fields. II. Poloidal fields, MNRAS, 163, 77.

Maumus, J., Bagdassarov, N. & Schmeling, H. (2005): Electrical conductivity and partial melting of mafic rocks under pressure. Geochim. Cosmochim. Acta. 69, p. 4703–4718.

Mayor, M., Queloz, D., (1995): A Jupiter-mass companion to a solar-type star. Nature 378 (November), 355–359.

McEwen, A. S. et al. (1998): High-temperature silicate volcanism on Jupiter's moon Io. Science 281, 87.

Melikian, ND et al. (2012): Spectral Detection of a very strong flare on WX UMa, in: HU ISSN 1587-2440, Information Bulletin on Variable Stars, No. 6031, 1.

Metzner J. & Schaal A. (2002): Schnelle Fourier-Transformation, Mathematische Ausarbeitung für das Fach "Seminar Numerische Mathematik" von Prof. Dr. Krautwald und Prof. Dr. Gleich, an der Fachhochschule München.

Morin, J. et al. (2010): Large-scale magnetic topologies of late M dwarfs, MNRAS, 407, 2269-2286.

Morin J. et al. (2010b): Large-scale magnetic topologies of mid M dwarfs, Monthly Notices of the Royal Astronomical Society, Volume 390, Issue 2, pp. 567-581.

Muirhead, P. S., Hamren, K., Schlawin, E., Rojas-Ayala, B., Covey, K. R., & Lloyd, J. P. (2012): ApJ, 750, L37.

Murray, C.D. & Dermott, S.F. (1999): Solar System Dynamics, Cambridge University Press.

Noack, L., Breuer, D. & Spohn, T. (2012): Coupling the atmosphere with interior dynamics: Implications for the resurfacing of Venus. Icarus 217, p. 484–498.

Noack, L., Rivoldini, A. and Van Hoolst, T. (2015): "CHIC - Coupling Habitability, Interior and Crust," INFOCOMP: Brussels, Belgium, vol. ISBN: 978-1-61208-416-9, pp. 84–90.

Noack, L., Rivoldini, A. & Van Hoolst, T. (2016): Modeling the evolution of terrestrial and water-rich planets and moons. Int. J. Adv. Syst. Meas. 9, 66–76.

Nutzman, P., & Charbonneau, D. (2008): Design Considerations for a Ground-Based Transit Search for Habitable Planets Orbiting M Dwarfs, PASP, 120, 317.

Pappalardo, R. T. et al. (1998): Geological evidence for solid-state convection in Europa's ice shell. Nature 391, 365–368.

Parkinson, W. D. (1983): Introduction to Geomagnetism, Scottish Academic Press, Edinburgh.

Patiño Douce, A. (2011). Energy sources in planetary bodies. In Thermodynamics of the Earth and Planets, pp. 70-121.

Pettersen, B. R. (1991): The nearby flare stars,Vol. 62, 217-242.

Peucker−Ehrenbrink, B., and G. Ravizza (2000), The effects of sampling artifacts on cosmic dust flux estimates: A reevaluation of nonvolatile tracers (Os, Ir), Geochim. Cosmochim. Acta, 64, p.1965–1970.

Pneuman, G.W. & Kopp, R.A.(1971): Gas-magnetic field interactions in the solar corona, Sol Phys. Vol. 18, Issue 2, p 258–270.
Pizzolato, N., Maggio, A., Micela, G., Sciortino, S., & Ventura, P. (2003): The stellar activity-rotation relationship revisited: Dependence of saturated and non-saturated X-ray emission regimes on stellar mass for late-type dwarfs, A&A, 397, 147.

Pravdo, S.H., Shaklan, S.B., Henry, T., and Benedict, G.Z. (2004) Astrometric discovery of GJ 164B. ApJ. 617, 1323–1329.

Pravdo, S.H., Shaklan, S.B., Lloyd, J., and Benedict, G.F. (2005) Discovering M-dwarf companions with STEPS. In Vol. CS-338: Astrometry in the Age of the Next Generation of Large Telescopes, edited by K. Seidelmann and A. Monet, Astronomical Society of the Pacific, San Francisco, in press.

Rauer, H., Catala, C., Aerts, C., et al. (2014): The PLATO 2.0 mission, Exp. Astron., 38, 249.

Reiners, A., & Basri, G. (2008): Chromospheric activity, rotation, and rotational braking in M and L dwarfs, ApJ, 684, 1390.

Reiners, A., & Basri, G. (2009): A Volume-Limited Sample of 63 M7-M9.5 Dwarfs. I. Space Motion, Kinematic Age, and Lithium, ApJ, Vol. 705, Issue 2, pp. 1416-1424.

Reiners, A. & Basri, G. A (2010): Volume-limited sample of 63 M7–M9.5 dwarfs. II. Activity, magnetism, and the fade of the rotation-dominated dynamo, ApJ. 710, 924–935.

Reiners, A. (2012): Observations of cool-star magnetic fields. Living Rev. Sol. Phys. 9, 1.

Rogers, L. A. (2015): Most 1.6 Earth-Radius Planets are not Rocky, ApJ, 801, 41.

Rubie, D. C., Melosh, H. J., Reid, J. E., Liebske, C., & Righter, K. (2003): Earth Planet. Sci. Lett., 205, p. 239.

Rudnev, V. (2003): Handbook of Induction Heating (Manufacturing, Engineering and Materials Processing) CRC Press.

Scalo, J., Kaltenegger, L., Segura, A. G., et al. (2007): M stars as targets for terrestrial exoplanet searches and biosignature detection, Astrobiology, 7, 85.

Schilling Nico, Fritz M. Neubauer, Joachim Saur (2007): Time-varying interaction of Europa with the jovian magnetosphere: Constraints on the conductivity of Europa's subsurface ocean, Icarus 192, 41–55.

Schmitt, J.H.M.M., Fleming, T.A., Giampapa, M.S. (1995): The X-Ray View of the Low-Mass Stars in the Solar Neighborhood, ApJ, 450, p. 392.

Schubert, G., Turcotte, D. L., & Olson, P. (2001): Mantle Convection in the Earth and Planets (Cambridge: Cambridge Univ. Press).

Schubert, G., Anderson, J. D., Spohn, T., and McKinnon, W. B. (2004). Interior Composition, Structure and Dynamics of the Galilean Satellites, pages 281– 306.

Schubert G. & K.M. Soderlund (2011): Planetary magnetic fields: Observations and models, Physics of the Earth and Planetary Interiors 187, 92–108.

Schwartz, K., Sonett, C. P., Colburn D. S. (1969): Unipolar induction in the moon and a lunar limb shock mechanism, The moon, Volume 1, Number 1, Page 7.

Seager S. (2013): Exoplanet Habitability, Science 340:577–581.

Seehafer, N. (1996): Nature of the α effect in magnetohydrodynamics. Physical Review E, 53(1), 1283.

Selsis, F., Kasting, J. F., Levrard, B., et al. (2007): Habitable planets around the star Gliese 581?, A&A, 476, 1373

Shirey, S. B., and S. H. Richardson (2011), Start of the Wilson cycle at 3 Ga shown by diamonds from subcontinental mantle, Science, 333(6041), 434–436.

Shulyak D. et al. (2015): Towards understanding dynamo action in M dwarfs, MNRAS 449 3471.

Shulyak D. et al. (2017): Strong dipole magnetic fields in fast rotating fully convective stars, Nature Astronomy, Vol. 1, id. 0184.

Silvestri, N. M., Hawley, S. L., & Oswalt, T. D. (2005): The chromospheric activity and ages of M dwarf stars in wide binary, AJ, 129, 2428.

Skumanich, A. (1972): Time Scales for CA II Emission Decay, Rotational Braking, and Lithium Depletion, ApJ, 171, 565.

Soffel, H. CR. (1991): Paläomagnetismus und Archäomagnetismus, Springer Verlag, 276 S., Berlin- Heidelberg-New York.

Solomatov, V. (1995): Scaling of temperature dependent and stress dependent viscosity convection, Phys. Fluids, 7, 266.

Solomon, S. C., & Head, J. W. (199): Fundamental issues in the geology and geophysics of venus. - NCBI, Science, 252, 252

Soderblom, D. R., Duncan, D. K., & Johnson, D. R. H. (1991): The chromospheric emission-age relation for stars of the lower main sequence and its implications for the star formation rate, ApJ, 375, 722.

Southam, G., Westall, F., & Spohn, T. (2015): Geology, Life, and Habitability, in Treatise on geophysics, ed. T. Spohn (Amsterdam: Elsevier), 10, p. 473.

Spencer J.R. and Schneider N.M., (1996): Io on the eve of Galileo mission, Annu. Rev. Earth Planet. Sci., 24, p. 125.

Spencer J.R., Jessup K.L., McGrath M.A., et al., (2000): Discovery of gaseous S2 in Io's pele plume, Science, 288, 1208.

Spencer, J. R., Rathbun, J. A., Travis, L. D., Tamppari, L. K., Barnard, L., Martin, T. Z., and McEwen, A. S. (2000). Io's Thermal Emission from the Galileo Photopolarimeter- Radiometer. Science, 288:1198–1201.

Srivastava, S. P. (1966): Theory of the magnetotelluric method for a spherical conductor. *Geophys. J.* **11**, p. 373–387.

Stamenković, V. & Breuer, D. (2014): The tectonic mode of rocky planets: Part 1–driving factors, models & parameters. Icarus 234, p. 174–193.

Stebbins; J. and Jacobsen, T. (1928): Luther photometric measures of Jupiter's satellites an Uranus, with tests for the solar constant. Lick Abs. Bull. 12, 180-195.

Steffl, A.J. et al. (2013): Cassini UVIS observations of the Io plasma torus. I. Initial results, Icarus, Volume 172, Issue 1, p. 78-90.

Stevenson, D.J. (2010): Planetary Magnetic Fields: Achievements and Prospects, Space Sci Rev, 152: 651.

Strom, R. G., et al. (1994): The global resurfacing of Venus, Journal of Geophysical Research; p. p. 10,899-10,926; (ISSN 0148-0227); 99; E5.

Stumpff, K. (1959): Himmelsmechanik, Band I, Hochschulbücher für Physik, Band 32 , VEB Deutscher Verlag der Wissenschaften, Berlin.

Tajika, E., & Matsui, T. (1992): Evolution of terrestrial proto-CO2 atmosphere coupled with thermal history of the earth, E&PSL, 113, 251.

Tajika, E. (2007): Long-term stability of climate and global glaciations throughout the evolution of the Earth, Earth Planets Space, 59, 293.

Tauxe, L. (2005): "Inclination flattening and the geocentric axial dipole hypothesis." Earth Planet. Sci. Lett. 233: 247-261.

Terasaki, H., Frost, D. J., Rubie, D. C., & Langenhorst, F. (2005): The effect of oxygen and sulphur on the dihedral angle between Fe–O–S melt and silicate minerals at high pressure: implications for Martian core formation, Earth Planet. Sci. Lett., 232, 379.

Tipler, P. A. (2004): Physik für Wissenschaftler und Ingenieure; Spektrum Akad. Verl., 1388 S., Heidelberg.

Tosi N. et al. (2017): The habitability of a stagnant-lid Earth, A&A 605, A71.

Turcotte, D. L. (1993): An episodic hypothesis for Venusian tectonics, Jour. Geophy. Res., Vol. 98, Issue E9.

Wagner, F., Tosi, N., Sohl, F., Rauer, H., Spohn, T. (2012): Rocky super-Earth interiors structure and internal dynamics of CoRoT-7b and Kepler-10b. Astron. Astro- phys. 541, A103.

Walker, J. C. G., Hays, P. B., & Kasting, J. F. (1981): A negative feedback mechanism for the long−term stabilization of Earth's surface temperature, J. Geophys. Res.: Oceans, 86, 9776.

Weigert A., H. J. Wendker, L. Wisotzki (2006): Astronomie und Astropyhsik, Wiley-VCH Verlag, 4. Auflage, 2006, p. 99-101.

West, A. A., Hawley, S. L., Bochanski, J. J., Covey, K. R., Reid, I. N., Dhital, S., Hilton, E. J., & Masuda, M. (2008): Constraining the age-activity relation for cool stars: the Sloan Digital Sky Survey Data Release 5 low-mass star spectroscopic sample, AJ, 135, 785.

West, Andrew A., Kolby L. Weisenburger, Jonathan Irwin, Zachory K. Berta-Thompson, David Charbonneau, Jason Dittmann, and J. Sebastian Pineda (2015): An Activity-Rotation Relationship and Kinematic Analysis of Nearby Mid-to-Late-Type M Dwarfs. The Astrophysical Journal 812, no. 1: 3.

West, A. A., et al. (2004): Spectroscopic properties of cool stars in the Sloan Digital Sky Survey: an analysis of magnetic activity and a search for subdwarfs, AJ, 128, 426.

Williams, P. K. G., Berger, E., Irwin, J., Berta-Thompson, Z. K.,& Charbonneau, D. (2014): Simultaneous Multiwavelength Observations of Magnetic Activity in Ultracool Dwarfs. IV.

The Active, Young Binary NLTT 33370 AB (= 2MASS J13142039+ 1320011), ApJ, Vol. 799, Nr. 2.

Wolf E. T. (2017): Assessing the Habitability of the TRAPPIST-1 System Using a 3D Climate Model, ApJL 839 L1.

Wolszczan, A., Frail, D. (1992): A planetary system around the millisecond pulsar psr1257 þ 12. Nature 355, p. 145–147.

Valencia, D., Sasselov, D. & O'Connell, R. J. (2007): Detailed Models of super-Earths: How well can we infer bulk properties?, ApJ, 656, p. 545.

Veeder, G. J., Matson, D. L., Johnson, T. V., Davies, A. G., and Blaney, D. L. (2004). The polar contribution to the heat flow of Io. Icarus, 169:264–270.

Vidotto, A. A., Jardine, M., Opher, M., Donati, J. F., & Gombosi, T. I. (2011b): Powerful winds from low-mass stars: V374 Peg, MNRAS, 412, 351.

Vidotto, A. A., Gregory, S. G., Jardine, M., et al. (2014): Stellar magnetism: empirical trends with age and rotation, MNRAS, 441, 2361.

Xu, Y., Shankland, T. J. & Poe, B. T. (2000): Laboratory-based electrical conductivity in the Earth's mantle. J. Geophys. Res. 105, p. 27.

Yade et al. (2016): Magnetic cycles in a dynamo simulation of the fully convective M-star Proxima Centauri, ApJL, 833:L28.

Yoshino, T., Matsuzaki, T., Yamashita, S. & Katsura, T. (2006): Hydrous olivine unable to account for conductivity anomaly at the top of the asthenosphere. Nature 443, p. 973–976.

Yoshino, T., Manthilake, G., Matsuzaki, T. & Katsura, T. (2008): Dry mantle transition zone inferred from the conductivity of wadsleyite and ringwoodite. Nature 451, p. 326–329.

Yoshino, T., Laumonier, M., McIsaac, E. & Katsura, T. (2010): Electrical conductivity of basaltic and carbonatite melt-bearing peridotites at high pressures: implications for melt distribution and melt fraction in the upper mantle. Earth. Planet. Sci. Lett. 295, p. 593–602.

Yoshino, T. & Katsura, T. (2013): Electrical conductivity of mantle minerals: role of water in conductivity anomalies. Annu. Rev. Earth. Planet. Sci. 41, p. 605–628.

Zahnle, K. J. and J. C. G. Walker (1982): The evolution of solar ultraviolet luminosity, Rev. Geophys., 20, 280–292.

Zendejas, J., Segura, A., & Raga, A. C. (2010): Atmospheric mass loss by stellar wind from planets around main sequence M stars, Icarus, 210, 539.

Zeng, L., & Seager, S. (2008): A computational tool to interpret the bulk composition of solid exoplanets based on mass and radius measurements, PASP, 120, 983.

Figures and tables